Naval Research Laboratory

Stennis Space Center, MS 39529-5004

NRL/FR/7322--00-9962

Description of the Navy Coastal Ocean Model Version 1.0

PAUL J. MARTIN

Ocean Dynamics and Prediction Branch
Oceanography Division

December 31, 2000

REPORT DOCUMENTATION PAGE

Form Approved
OMB No. 0704-0188

1. AGENCY USE ONLY (*Leave Blank*)	2. REPORT DATE	3. REPORT TYPE AND DATES COVERED
	December 31, 2000	Interim

4. TITLE AND SUBTITLE

Description of the Navy Coastal Ocean Model Version 1.0

5. FUNDING NUMBERS

PE - 0602435N
WU - DN15-3077

Funding Document Number:
N001401WX20609

6. AUTHOR(S)

Paul J. Martin

7. PERFORMING ORGANIZATION NAME(S) AND ADDRESS(ES)

Naval Research Laboratory
Stennis Space Center, MS 39529-5004

8. PERFORMING ORGANIZATION REPORT NUMBER

NRL/FR/7322--00-9962

9. SPONSORING/MONITORING AGENCY NAME(S) AND ADDRESS(ES)

Office of Naval Research
800 North Quincy Street
Arlington, VA 22217-5660

10. SPONSORING/MONITORING AGENCY REPORT NUMBER

11. SUPPLEMENTARY NOTES

12a. DISTRIBUTION/AVAILABILITY STATEMENT

Approved for public release; distribution is unlimited.

12b. DISTRIBUTION CODE

13. ABSTRACT (*Maximum 200 words*)

This report provides a description of the Navy Coastal Ocean Model (NCOM) Version 1.0. The model has a free surface and is based on the primitive equations and the hydrostatic, Boussinesq, and incompressible approximations. The model uses an Arakawa C grid, is leapfrog in time with an Asselin filter to suppress timesplitting, and uses second-order centered spatial finite differences. The propagation of surface waves and vertical diffusion is treated implicitly. A choice of the Mellor-Yamada Level 2 or Level 2.5 turbulence models is provided for the parameterization of vertical mixing.

The horizontal grid is curvilinear. The vertical grid uses sigma coordinates for the upper layers and z-level (constant depth) coordinates for the lower layers, and the depth at which the model changes from sigma to z-level coordinates can be specified by the user. The combined vertical coordinate system provides some flexibility in setting up the vertical grid and easily allows comparisons to be made between simulations conducted with sigma and z-level coordinates. The inclusion of a source term in the model equations simplifies input of river and runoff inflows. Some limitations of the model are discussed.

14. SUBJECT TERMS

Ocean model
Coastal
Ocean modeling

15. NUMBER OF PAGES

45

16. PRICE CODE

17. SECURITY CLASSIFICATION OF REPORT	18. SECURITY CLASSIFICATION OF THIS PAGE	19. SECURITY CLASSIFICATION OF ABSTRACT	20. LIMITATION OF ABSTRACT
UNCLASSIFIED	UNCLASSIFIED	UNCLASSIFIED	UL

NSN 7540-01-280-550

Standard Form 298 (Rev. 2-89)
Prescribed by ANSI Std 239-18
298-102

CONTENTS

DESCRIPTION OF THE NAVY COASTAL OCEAN MODEL VERSION 1.0

1. INTRODUCTION

This report presents a description of the Navy Coastal Ocean Model (NCOM) Version 1.0. The report discusses the physics and numerics of the model and some of its limitations.

The goals in developing NCOM were to provide an ocean model that would include the best features of existing ocean models, would meet the Navy's needs for coastal ocean simulation and prediction, and would be fully compatible with and could be fully coupled with the Navy's Coupled Ocean and Atmospheric Mesoscale Prediction System (COAMPS) (Hodur 1997).

The first of these goals is somewhat elusive in that new ocean model features are continually being developed within the ocean modeling community. The approach taken for the initial development of NCOM 1.0 is to make use of fairly well-established ocean modeling techniques that have been demonstrated to work well and to incorporate improvements and additional capabilities into NCOM when they are determined to be useful or needed. Also, it may not be possible to meet all the Navy's coastal modeling needs with a single model. However, the approach is to make NCOM as flexible as possible without incurring a significant penalty in terms of efficiency.

COAMPS was developed by the Marine Meteorology Division of the Naval Research Laboratory (NRL) at Monterey, California, and has a very specific code structure that provides for calls to (i.e., coupling between) both the atmospheric and ocean models within the same Fortran program. COAMPS also provides for an arbitrary number of levels of nesting within the same Fortran program. This nesting capability is made possible by using dynamic memory allocation with array dimensions specified at run time and by passing model variables to subroutines through subroutine argument lists rather than through common blocks. This allows the same model routines to calculate the different nests. Since most ocean models are not structured in this way, a certain amount of recoding is required to fully adapt an existing ocean model to the COAMPS code structure.

NCOM Version 1.0 is based primarily on two existing ocean models, the Princeton Ocean Model (POM) and the Sigma/Z-level Model (SZM). POM was developed by Alan Blumberg and George Mellor (Blumberg and Mellor 1983; Blumberg and Mellor 1987). POM is well-known to anyone familiar with ocean models and has attracted a wide base of users within the academic, civilian, and government communities. Table 1 lists some of the main features of POM. POM is a three-dimensional (3-D), primitive equation, baroclinic, hydrostatic, free surface model and uses an orthogonal-curvilinear horizontal grid, a sigma (i.e., bottom-following) vertical grid, a split-explicit treatment of the free surface, Smagorinsky horizontal mixing, and the Mellor-Yamada Level 2.5 (MYL2.5) turbulence model for vertical mixing.

Manuscript approved August 3, 1998.

Table 1 — Comparison of Features of POM and SZM

POM	*SZM*
Primitive Equation	Primitive Equation
Incompressible	Incompressible
Hydrostatic	Hydrostatic
Boussinesq	Boussinesq
Free Surface	Free Surface
Smagorinsky Horizontal Mixing	Grid-Cell Re Number Horizontal Mixing
Mellor-Yamada Level 2.5 Vertical Mixing	Mellor-Yamada Level 2 Vertical Mixing
Quadratic Bottom Drag	Quadratic Bottom Drag
Curvilinear Horizontal Grid	Cartesian Horizontal Grid
Sigma Coordinate Vertical Grid	Combined Sigma/Z-level Vertical Grid
Leapfrog in Time with Asselin Filter	Leapfrog in Time with Asselin Filter
Second-Order, Centered Finite Differences	Second-Order, Centered Finite Differences
Flux Conservative Formulation	Flux Conservative Formulation
Split-Explicit Treatment of Free Surface	Implicit Treatment of Free Surface
Implicit Vertical Mixing	Implicit Vertical Mixing

SZM was developed in-house at NRL, Stennis Space Center, MS (Martin et al. 1998). SZM is similar in many ways to POM (see Table 1) but differs from POM in that it uses a Cartesian horizontal grid (the grid spacing in the horizontal is constant), a combined sigma/z-level vertical grid with sigma layers near the surface and z-levels (i.e, fixed-depth levels) below a user-specified depth, an implicit treatment of the free surface, horizontal eddy coefficients calculated based on a maximum grid-cell Reynolds number criteria, and vertical eddy coefficients calculated using the Mellor-Yamada Level 2 (MYL2) turbulence closure scheme.

In a coastal model comparison study that was conducted at NRL (Martin et al. 1998), POM and SZM were found to simulate a number of basic physical processes that are important in the coastal ocean (advection, mixing, and the propagation of surface, internal, and coastal trapped waves) fairly well.

NCOM uses those features of POM and SZM that tend to provide the most flexibility and provides a choice in many cases where selection of one scheme or parameterization over another is difficult because of trade-offs that can be situation dependent. The horizontal grid is orthogonal-curvilinear as in POM, which allows adaptation to different map projections and also allows for use of a limited amount of grid curvature to follow a slowly curving coastline or bathymetric feature and/or to provide increased grid resolution in certain areas of the domain. The sigma/z-level vertical grid from SZM is used to offer a choice of sigma layers or z-levels, or some combination with sigma layers in the shallow water and z-levels in the deeper water. A choice of grid-cell Reynolds number or Smagorinsky horizontal diffusion and MYL2 or MYL2.5 vertical diffusion is provided.

The free surface is treated implicitly as in SZM. This is significantly simpler than the split-explicit scheme used in POM and is more consistent in the sense that the depth-averaged equations are the almost exact vertical integral of the 3-D equations. However, the implicit scheme is not

as accurate for the propagation of surface gravity waves because of the much larger timestep used to propagate these waves (for some comparisons, see Martin et al. 1998). However, an implicit treatment of the free surface has been used in a number of coastal models (Leendertse 1989; Blumberg 1992; Casulli and Cattani 1994; Casulli and Cheng 1994). An implicit treatment of the free surface has usually been found to be sufficiently accurate to simulate tides and wind setup since the length and time scales of these processes are relatively long. It was originally planned to offer a choice of an implicit or split-explicit treatment of the free surface. However, there are some inconsistencies between the use of a split-explicit scheme and a z-level type of grid that have not yet been resolved. The option of a split-explicit treatment of the free surface may be provided at a later time.

Some additional features of NCOM are (1) a source term in all the equations to simplify input of rivers and coastal runoff, (2) the option of including forcing by the surface air pressure and the tidal potential, (3) a multicomponent scalar variable array that allows additional scalar fields to be easily added to the model (e.g., for optical or biological submodels), (4) shrink-wrapping to eliminate calculations over land points on the left and right sides of the domain, and (5) slabwise calculation through the model grid to improve the use of high-speed cache memory.

The sections that follow include (2) a description of the model physics, (3) a description of the model numerics, (4) a discussion of the limitations of the model, (5) a discussion of some plans for future development of NCOM, and (6) a summary.

2. MODEL PHYSICS

2.1 Basic Equations

The ocean model is free surface and employs the hydrostatic, Boussinesq, and incompressible approximations. The equations that are solved, written in Cartesian coordinates, are

$$\frac{\partial u}{\partial t} = -\nabla \cdot (\mathbf{v}u) + Qu + fv - \frac{1}{\rho_o}\frac{\partial p}{\partial x} + F_u + \frac{\partial}{\partial z}\left(K_M \frac{\partial u}{\partial z}\right), \tag{1}$$

$$\frac{\partial v}{\partial t} = -\nabla \cdot (\mathbf{v}v) + Qv - fu - \frac{1}{\rho_o}\frac{\partial p}{\partial y} + F_v + \frac{\partial}{\partial z}\left(K_M \frac{\partial v}{\partial z}\right), \tag{2}$$

$$\frac{\partial p}{\partial z} = -\rho g, \tag{3}$$

$$\frac{\partial u}{\partial x} + \frac{\partial v}{\partial y} + \frac{\partial w}{\partial z} = Q, \tag{4}$$

$$\frac{\partial T}{\partial t} = -\nabla \cdot (\mathbf{v}T) + QT + \nabla_h (A_H \nabla_h T) + \frac{\partial}{\partial z}\left(K_H \frac{\partial T}{\partial z}\right) + Q_r \frac{\partial \gamma}{\partial z}, \tag{5}$$

$$\frac{\partial S}{\partial t} = -\nabla \cdot (\mathbf{v}S) + QS + \nabla_h (A_H \nabla_h S) + \frac{\partial}{\partial z}\left(K_H \frac{\partial S}{\partial z}\right), \tag{6}$$

$$\rho = \rho(T, S, z), \tag{7}$$

where t is the time; x, y, and z are the three coordinate directions; u, v, and w are the three components of the velocity vector; Q is a volume flux source term; $\mathbf{v}$ is the vector velocity; T is the potential temperature; S is the salinity; ∇_h is the horizontal gradient operator; f is the Coriolis parameter; p is the pressure; ρ is the water density; ρ_o is a reference water density; g is the acceleration of gravity; F_u and F_v are horizontal mixing terms for momentum; A_H is the horizontal mixing coefficient for scalar fields (temperature and salinity); K_M and K_H are vertical eddy coefficients for momentum and scalar fields, respectively; Q_r is the solar radiation; and γ is a function describing the solar extinction.

Density ρ must be calculated from T and S using a suitable equation of state. Two equations of state are provided within NCOM, the polynomial equation of state of Friedrich and Levitus (1972) and the United Nations Educational, Scientific, and Cultural Organization (UNESCO) formula as adapted by Mellor (1991) for use in POM.

2.2 Surface and Bottom Boundary Conditions

Equations (1) to (6) are subject to boundary conditions in the form of fluxes and stresses at the ocean's surface and bottom. The boundary conditions at the surface at $z = \zeta$, which are due to fluxes between the ocean and the atmosphere, are

$$K_M \frac{\partial u}{\partial z} = \frac{\tau^x}{\rho_o}, \tag{8}$$

$$K_M \frac{\partial v}{\partial z} = \frac{\tau^y}{\rho_o}, \tag{9}$$

$$K_H \frac{\partial T}{\partial z} = \frac{Q_b + Q_e + Q_s}{\rho_o c_p}, \tag{10}$$

$$K_H \frac{\partial S}{\partial z} = S|_{z=\zeta}(E_v - P_r), \tag{11}$$

where τ^x and τ^y are the x and y components of the surface wind stress, Q_b, Q_e, and Q_s are the net longwave and latent and sensible surface heat fluxes, E_v and P_r are the surface evaporation and precipitation rates, and c_p is the specific heat of seawater. At the ocean bottom at $z = H$, the boundary conditions are

$$K_M \frac{\partial u}{\partial z} = c_b u|\mathbf{v}|, \tag{12}$$

$$K_M \frac{\partial v}{\partial z} = c_b v|\mathbf{v}|, \tag{13}$$

$$K_H \frac{\partial T}{\partial z} = 0, \tag{14}$$

$$K_H \frac{\partial S}{\partial z} = 0. \tag{15}$$

The bottom stress is parameterized here by a quadratic drag law with drag coefficient c_b. The value of c_b can be specified or calculated in terms of the bottom layer thickness Δz_b and the bottom roughness z_o as

$$c_b = \max \left[\frac{\kappa^2}{\log^2(\frac{\Delta z_b}{2z_o})}, c_{b_{min}} \right], \tag{16}$$

where $\kappa = 0.4$ is von Karman's constant, and $c_{b_{min}}$ is a minimum value for c_b. This expression for c_b is derived by assuming a logarithmic boundary layer velocity profile near the bottom.

2.3 Horizontal Pressure Gradient

Integration of the hydrostatic Eq. (3) in the vertical from a depth z to the surface at $z = \zeta$ yields

$$\int_z^\zeta \frac{\partial p}{\partial z} dz = -g \int_z^\zeta \rho dz. \tag{17}$$

The vertical pressure gradient integrates exactly to give

$$p(\zeta) - p(z) = -g \int_z^\zeta \rho dz. \tag{18}$$

Taking a horizontal derivative (e.g., in x) and using Leibnitz's rule for the differentiation of an integral,

$$\frac{\partial p(\zeta)}{\partial x} - \frac{\partial p}{\partial x} = -g\rho(\zeta)\frac{\partial \zeta}{\partial x} - g \int_z^\zeta \frac{\partial \rho}{\partial x} dz. \tag{19}$$

Taking $\rho(\zeta) \simeq \rho_o$, dividing by ρ_o, and rearranging terms, the expression for the Boussinesq horizontal pressure gradient in x is

$$\frac{1}{\rho_o}\frac{\partial p}{\partial x} = \frac{1}{\rho_o}\frac{\partial p(\zeta)}{\partial x} + g\frac{\partial \zeta}{\partial x} + \frac{g}{\rho_o}\int_z^\zeta \frac{\partial \rho}{\partial x} dz. \tag{20}$$

The first term on the right side of Eq. (20) is the pressure gradient at the surface (i.e., the surface atmospheric pressure gradient), the second term is the horizontal pressure gradient due to differences in the surface elevation, and the third term is the horizontal pressure gradient due to the density field, which is sometimes referred to as the baroclinic pressure gradient. The horizontal pressure gradient in y is calculated in similar fashion.

2.4 Horizontal Mixing

The model uses the Laplacian form of horizontal mixing, and two horizontal mixing parameterizations are provided. One is based on maintaining a maximum horizontal grid-cell Reynolds number, and the other is the Smagorinsky scheme (Smagorinsky 1963), which is used in POM.

For the grid-cell Reynolds number scheme, the horizontal friction terms in the momentum equations use the form

$$F_u = \frac{\partial}{\partial x}\left(A_M \frac{\partial u}{\partial x}\right) + \frac{\partial}{\partial y}\left(A_M \frac{\partial u}{\partial y}\right), \tag{21}$$

$$F_v = \frac{\partial}{\partial x}\left(A_M \frac{\partial v}{\partial x}\right) + \frac{\partial}{\partial y}\left(A_M \frac{\partial v}{\partial y}\right). \tag{22}$$

The horizontal mixing coefficient A_M is set equal to the maximum of a constant background value A_o and a value needed to keep the grid-cell Reynolds Number R_{e_g} below a maximum specified value, i.e., in the x-direction,

$$A_M = \max\left[A_o, \frac{|u|\Delta x}{R_{e_g}}\right], \tag{23}$$

and in the y-direction

$$A_M = \max\left[A_o, \frac{|v|\Delta y}{R_{e_g}}\right], \tag{24}$$

where Δx and Δy are the horizontal grid spacing in x and y, respectively. The value of R_{e_g} is typically set to a value in the range of 10 to 100.

For the Smagorinsky mixing scheme, the horizontal friction terms have the form

$$F_u = \frac{\partial}{\partial x}\left(2A_M \frac{\partial u}{\partial x}\right) + \frac{\partial}{\partial y}\left(A_M \left(\frac{\partial u}{\partial y} + \frac{\partial v}{\partial x}\right)\right), \tag{25}$$

$$F_v = \frac{\partial}{\partial y}\left(2A_M \frac{\partial v}{\partial y}\right) + \frac{\partial}{\partial x}\left(A_M \left(\frac{\partial u}{\partial y} + \frac{\partial v}{\partial x}\right)\right). \tag{26}$$

The horizontal mixing coefficient A_M is calculated as a function of the local horizontal grid resolution and velocity shear, i.e.,

$$A_M = C_{smag}\Delta x \Delta y \left(\left(\frac{\partial u}{\partial x}\right)^2 + \frac{1}{2}\left(\frac{\partial v}{\partial x} + \frac{\partial u}{\partial y}\right)^2 + \left(\frac{\partial v}{\partial y}\right)^2\right)^{\frac{1}{2}}. \tag{27}$$

The magnitude of the Smagorinsky eddy coefficient calculation is scaled by the constant C_{smag}. Values used for C_{smag} range from about 0.02 to 0.5. Large values of C_{smag} tend to dissipate smaller features, whereas values that are too small can lead to excessive numerical noise and/or instability. A typical value that is used is 0.1.

The grid-cell Reynolds number scheme is simpler and, with the mixing coefficients scaled according to the velocity magnitude, is specifically geared toward suppressing noise generated by numerical advection. The Smagorinsky scheme scales the rate of mixing according to the horizontal velocity shear and might be considered to be more physically based. The eddy coefficients calculated by the Smagorinsky scheme are isotropic and are independent of coordinate rotation; those calculated by the grid-cell Reynolds number method are not.

The form used for horizontal diffusion of T and S is the Laplacian form expressed in Eqs. (5) and (6). NCOM provides for allowing A_H to be some fraction of A_M via specification of an inverse Prandtl Number. Setting $A_H = A_M$ is a common choice, but for some applications it may be desirable to set A_H different from A_M.

2.5 Vertical Mixing

The vertical eddy coefficients are specified as

$$K_M = \max\left[K_{M_0}, K_{M_1}, K_{M_2}, \frac{|w|\Delta z}{R_{e_z}}\right], \tag{28}$$

$$K_H = \max\left[K_{H_0}, K_{H_1}, K_{H_2}, \frac{|w|\Delta z}{R_{e_z}}\right], \tag{29}$$

where K_{M_0} and K_{H_0} are small, background values, K_{M_1} and K_{H_1} are calculated from a turbulence model, K_{M_2} and K_{H_2} parameterize turbulent mixing by unresolved processes at near-critical Richardson Numbers (Large et al. 1994), Δz is the vertical grid spacing, and R_{e_z} is a maximum grid-cell Reynolds number for the vertical direction.

The background values K_{M_0} and K_{H_0} are constants. Their purpose is to parameterize weak, vertical mixing processes that are not accounted for by the other mixing parameterizations. They are generally kept quite small since large values would be unrealistic and would excessively erode the stratification and damp the flow, especially in shallow water. Typical values are 10^{-5} m^2/s or less.

Two turbulence schemes are provided for calculating K_{M_1} and K_{H_1}, the MYL2.5 scheme (Mellor and Yamada 1982; Mellor 1996), which is used in POM, and the simpler MYL2 scheme (Mellor and Yamada 1974; Mellor and Durbin 1975). In both of these schemes, K_{M_1} and K_{H_1} are calculated as

$$K_{M_1} = \ell q S_M, \tag{30}$$

$$K_{H_1} = \ell q S_H, \tag{31}$$

where ℓ is a vertical turbulent length scale, $\frac{1}{2}q^2$ is the turbulent kinetic energy (TKE), and S_M and S_H are stratification functions that describe the effect of stratification on the vertical mixing.

The MYL2.5 scheme provides a prognostic equation to calculate the TKE that includes advective and diffusive transport. Another prognostic equation for the quantity $q^2\ell$ is used to provide an estimate for the vertical turbulence length scale ℓ. These two equations are

$$\begin{aligned}\frac{\partial q^2}{\partial t} = &-\nabla\cdot(\mathbf{v}q^2) + Qq^2 + \nabla_h(A_H\nabla_h q^2) + \frac{\partial}{\partial z}\left(K_{q_1}\frac{\partial q^2}{\partial z}\right)\\ &+ 2K_{M_1}\left(\left(\frac{\partial u}{\partial z}\right)^2 + \left(\frac{\partial v}{\partial z}\right)^2\right) + 2\frac{g}{\rho_o}K_{H_1}\left(\frac{\partial\tilde{\rho}}{\partial z}\right) - \frac{2q^3}{b_1\ell},\end{aligned} \tag{32}$$

$$\begin{aligned}\frac{\partial q^2\ell}{\partial t} = &-\nabla\cdot(\mathbf{v}q^2\ell) + Qq^2\ell + \nabla_h(A_H\nabla_h q^2\ell) + \frac{\partial}{\partial z}\left(K_{q_1}\frac{\partial q^2\ell}{\partial z}\right)\\ &+ E_1\ell\left(K_{M_1}\left(\left(\frac{\partial u}{\partial z}\right)^2 + \left(\frac{\partial v}{\partial z}\right)^2\right) + \frac{E_3 g}{\rho_o}K_{H_1}\left(\frac{\partial\tilde{\rho}}{\partial z}\right)\right) - \frac{q^3}{b_1}W,\end{aligned} \tag{33}$$

where

$$W = 1 + E_2 \left(\frac{\ell}{\kappa L} \right)^2, \tag{34}$$

$$L^{-1} = (\zeta - z + z_s)^{-1} + (z - H + z_o)^{-1}, \tag{35}$$

$$\frac{\partial \tilde{\rho}}{\partial z} = \frac{\partial \rho}{\partial z} - c_s^{-2} \frac{\partial p}{\partial z}. \tag{36}$$

In the above equations, K_{q_1} is the vertical diffusion coefficient for q^2 and $q^2\ell$, which is taken to be proportional to K_{H_1} ($K_{q_1} = 0.41 K_{H_1}$), z_s is the surface roughness, c_s is the speed of sound, and b_1, E_1, E_2, and E_3 are constants (see Table 2).

As discussed by Mellor and Yamada (1982), Eq. (33), which is used to obtain the turbulence length scale, is somewhat ad hoc. Most of the methods used to estimate turbulence length scales resort to some degree of empiricism.

Mellor and Yamada (1982) refer to W as a "wall-proximity" function, which is used to scale ℓ near the surface and bottom. This function has been modified from the form used in POM to account for the surface roughness length z_s and the bottom roughness length z_o (in POM, L in Eq. (35) tends to zero at the top and bottom). Since z_s and z_o are usually fairly small relative to the vertical grid resolution, the effect of this change is not usually significant. However, in the case of strong winds and breaking waves at the surface, the surface roughness can significantly increase the mixing in the surface mixed layer (Craig and Banner 1994; Craig 1996).

Table 2 — Constants for MYL2.5 Turbulence Model

parameter	*value*
a_1	0.92
a_2	0.74
b_1	16.6
b_2	10.1
c_1	0.08
E_1	1.8
E_2	1.33
E_3	1.0

The density $\tilde{\rho}$, which is used to calculate the vertical buoyancy gradient in the TKE equation, must not include the effect of local changes in pressure on the density; otherwise, the vertical stability will be overestimated. If ρ is calculated as an in situ density, where the effect of pressure on the density is accounted for, Eq. (36) provides the correction to remove the effect of local pressure changes on the vertical density gradient. If the model density does not include the effect of pressure, one can set $\tilde{\rho} = \rho$ (in shallow water, the effects of pressure on the density are small and are often neglected).

Prognostic Eqs. (32) and (33) require boundary conditions at the surface and bottom. At the surface at $z = \zeta$, the boundary conditions are given by

$$q^2 = b_1^{\frac{2}{3}} \left(\frac{\tau}{\rho_o} \right), \tag{37}$$

$$q^2 \ell = b_1^{\frac{2}{3}} \left(\frac{\tau}{\rho_o} \right) \kappa z_s. \tag{38}$$

NCOM also provides the option of specifying the flux of TKE at the surface rather than the value itself. The surface TKE flux is currently parameterized in terms of the surface wind stress, i.e., at $z = \zeta$

$$K_M \frac{\partial q^2}{\partial z} = c_{wave} \left(\frac{\tau}{\rho_o} \right)^{\frac{3}{2}}, \tag{39}$$

where c_{wave} is a constant that scales the TKE input from the waves. (Note that if wave data are available, it might be preferable to parameterize the surface TKE flux in terms of the actual sea state.) This boundary condition for the surface TKE flux, along with accounting for the surface roughness due to surface waves, allows for the simulation of the wave-mixing layer near the surface in which there is enhanced mixing from the energy input from breaking waves (Craig and Banner 1994).

At the bottom at $z = H$, the boundary conditions are

$$q^2 = b_1^{\frac{2}{3}} c_b (u^2 + v^2)^{\frac{1}{2}}, \tag{40}$$

$$q^2 \ell = b_1^{\frac{2}{3}} c_b (u^2 + v^2)^{\frac{1}{2}} \kappa z_o. \tag{41}$$

The stratification functions S_M and S_H are calculated as

$$S_H = \frac{C_1}{1 - C_2 G_H}, \tag{42}$$

$$S_M = \frac{C_3 + C_4 S_H}{1 - C_5 G_H}, \tag{43}$$

where

$$G_H = \min \left[0.028, \frac{\ell^2 g}{q^2 \rho_o} \frac{\partial \tilde{\rho}}{\partial z} \right]. \tag{44}$$

The constants C_1 – C_5 are calculated from the basic turbulence constants (a_1, a_2, b_1, b_2, and c_1) as

$$C_1 = a_2 (b_1 - 6a_1)/b_1, \tag{45}$$

$$C_2 = a_2 (18a_1 + 3b_2), \tag{46}$$

$$C_3 = a_1 (b_1 (1 - 3C_1) - 6a_1)/b_1, \tag{47}$$

$$C_4 = a_1(18a_1 + 9a_2), \tag{48}$$

$$C_5 = 9a_1a_2. \tag{49}$$

Table 2 lists the values of the constants used in the MYL2.5 turbulence model.

The MYL2 turbulence model assumes that there is approximately a local balance between shear production, buoyancy production, and dissipation in the TKE equation (these are the last three terms in Eq. (32)). With this assumption, q can be calculated algebraically from the mean vertical density and velocity gradients

$$q = \ell \left(b_1 \left(S_M \left(\left(\frac{\partial u}{\partial z} \right)^2 + \left(\frac{\partial v}{\partial z} \right)^2 \right) + S_H \frac{g}{\rho_o} \frac{\partial \tilde{\rho}}{\partial z} \right) \right)^{\frac{1}{2}}. \tag{50}$$

An empirical formulation is used to estimate ℓ. The turbulent length scale ℓ is set to zero outside of turbulent layers, and within a turbulent layer is scaled as the vertical distance to the edge of the turbulent layer, i.e., if z_t is the distance to the top of the turbulent layer and z_b is the distance to the bottom of the turbulent layer, then the local turbulent length scale ℓ within the turbulent layer is calculated as

$$\ell = \kappa(z_t^{-1} + z_b^{-1})^{-1}. \tag{51}$$

In the surface mixed layer, the surface roughness is added to z_t, and in the bottom boundary layer the bottom roughness is added to z_b so that the value of ℓ reflects the surface and bottom roughness. Calculated from Eq. (51), ℓ has a quadratic profile within a turbulent layer, and the value of ℓ at the center of a turbulent layer is about 10% of the thickness of the layer (for small values of z_s and z_o). This is a somewhat crude parameterization of ℓ, but this is mitigated somewhat by the fact that the depth of turbulent layers predicted by the MYL2 scheme in density stratified conditions tends to be only weakly dependent on the value of ℓ. There is also the point that more elaborate turbulence parameterizations frequently do not describe the details of turbulent mixing very well since they do not account for or adequately resolve some of the significant processes.

The stratification functions S_M and S_H for MYL2 are calculated from the Richardson Number R_i as

$$S_H = C_1' - C_2' R, \tag{52}$$

$$S_M = S_H \frac{C_3' - C_4' R}{C_5' - C_6' R}, \tag{53}$$

where

$$R = \frac{R_f}{1 - R_f}, \tag{54}$$

$$R_f = C_7' + C_8' R_i - ((C_8'^2 R_i + C_9') R_i + C_7'^2)^{\frac{1}{2}}, \tag{55}$$

$$C_1' = a_2(b_1 - 6a_1)/b_1, \tag{56}$$

$$C_2' = a_2(18a_1 + 3b_2)/b_1, \tag{57}$$

$$C_3' = a_1(b_1(1 - 3c_1) - 6a_1)/a_2, \tag{58}$$

$$C_4' = a_1(18a_1 + 9a_2)/a_2, \tag{59}$$

$$C_5' = b_1 - 6a_1, \tag{60}$$

$$C_6' = 9a_1 + 3b_2, \tag{61}$$

$$C_7' = \frac{1}{2}\frac{C_3'}{C_3' + C_4'}, \tag{62}$$

$$C_8' = \frac{1}{2}\frac{C_5' + C_6'}{C_3' + C_4'}, \tag{63}$$

$$C_9' = 2C_7'C_8' - \frac{C_5'}{C_3' + C_4'}. \tag{64}$$

In these equations, R_f is a flux Richardson Number ($R_f = R_i K_H/K_M = R_i S_H/S_M$), and a_1, a_2, b_1, b_2, and c_1 are the the same basic turbulence constants as used for the MYL2.5 model. Table 3 lists the values for the constants used for the MYL2 turbulence model. Note that the basic turbulence constants used here for the MYL2 model are as used by Mellor and Durbin (1975) and are slightly different from the values used in the MYL2.5 model.

Table 3 — Constants for MYL2 Turbulence Model

parameter	*value*
a_1	0.78
a_2	0.78
b_1	15.0
b_2	8.0
c_1	0.056

The MYL2 turbulence model as described here was compared with the MYL2.5 scheme as used in POM for some simple cases of surface-layer mixing by winds and heat fluxes and bottom-layer mixing by tidal currents and was found to give similar turbulence mixing scales and similar turbulent layer depths for these cases (Martin 1985; Martin 1986; Martin et al. 1998). Because of its simplicity, the MYL2 turbulence model is relatively efficient and does not carry the computational burden of the MYL2.5 scheme, which requires the model to carry and calculate two additional

prognostic variables. However, the MYL2.5 scheme has some advantages. For example, in high-resolution simulations, transport of TKE will be more significant and the assumption of local equilibrium of turbulence by the MYL2 model may be less accurate. Also, because it does not account for vertical diffusion of TKE, the MYL2 model cannot simulate the wave mixing layer that occurs near the surface in strong winds.

Tests of upper-ocean mixing in the open ocean with turbulence models such as MYL2 and MYL2.5 have frequently found that the models do not predict as much mixing as is observed (Martin 1985; Large et al. 1994; Kantha and Clayson 1994). It has been hypothesized that this is due, not so much to the fact that the mixing mechanisms in these models are incorrect, but that many mixing processes are not accounted for in these simulations, including many sources of background shear (internal waves, inertial gravity wave pumping, etc.) and Langmuir circulations.

NCOM provides an option to include the vertical mixing enhancement scheme of Large et al. (1994). The purpose of this mixing scheme is to account for unresolved mixing processes by extending the mixing of typical oceanic turbulence models above the normal critical Richardson number value of 0.2 to 0.5. The Large et al. enhancement scheme extends the mixing to $R_i = 0.7$ and is described by

$$K_{M_2} = K_{H_2} = \begin{array}{lll} K_o & & R_i < 0 \\ K_o(1-(R_i/0.7)^2)^3 & 0 < R_i & < 0.7 \\ 0 & & R_i > 0.7, \end{array}$$

where $K_o = 50$ cm^2/s. This scheme was utilized by Large et al. in conjunction with an adaptation of the atmospheric boundary layer model of Troen and Mahrt (1986) and by Kantha and Clayson (1994) in conjunction with the MYL2.5 turbulence closure model. Both Large et al. and Kantha and Clayson found that the addition of this mixing improved agreement of predictions of the ocean surface mixed layer with observations from several open-ocean data sets. However, it is not clear whether such a mixing enhancement is needed in shallow, coastal water.

2.6 Vertically Averaged Equations

The depth-averaged momentum and continuity equations are needed to calculate the free-surface mode in the model. Substituting the form of the horizontal pressure gradient from Eq. (20) into the momentum Eqs. (1) and (2) and integrating from the bottom to the surface gives the form of the momentum equations used for the calculation of the free-surface mode

$$\frac{\partial D\overline{u}}{\partial t} = -gD\frac{\partial \zeta}{\partial x} + \int_H^\zeta G_u dz, \tag{65}$$

$$\frac{\partial D\overline{v}}{\partial t} = -gD\frac{\partial \zeta}{\partial y} + \int_H^\zeta G_v dz, \tag{66}$$

where D is the total depth ($D = \zeta - H$), $\overline{u}$ and $\overline{v}$ are the depth-averaged horizontal velocities, and $\overline{Q}$ is the depth-averaged mass flux source term, and

$$G_u = -\nabla\cdot(\mathbf{v}u) + Qu + fv - \frac{1}{\rho_o}\frac{\partial p(\zeta)}{\partial x} - \frac{g}{\rho_o}\int_z^\zeta \frac{\partial \rho}{\partial x}dz + F_u + \frac{\partial}{\partial z}\left(K_M\frac{\partial u}{\partial z}\right), \tag{67}$$

$$G_v = -\nabla \cdot (\mathbf{v}v) + Qv - fu - \frac{1}{\rho_o}\frac{\partial p(\zeta)}{\partial y} - \frac{g}{\rho_o}\int_z^\zeta \frac{\partial \rho}{\partial y}dz + F_v + \frac{\partial}{\partial z}\left(K_M \frac{\partial v}{\partial z}\right). \tag{68}$$

The depth-integrated continuity equation is

$$\frac{\partial \zeta}{\partial t} = -\frac{\partial (D\overline{u})}{\partial x} - \frac{\partial (D\overline{v})}{\partial y} + D\overline{Q}. \tag{69}$$

3. MODEL NUMERICS

3.1 Horizontal Grid

The model uses an orthogonal, curvilinear, horizontal grid as used in POM, which allows adaptation of the grid to different map projections and also allows the grid to be set up with some mild curvature. The form of the model's equations in orthogonal, curvilinear, horizontal coordinates is presented in Appendix A. As a practical matter, the main differences from the Cartesian equations with constant grid spacing in x and y with regard to converting the equations to finite difference form are (1) the horizontal grid-cell dimensions in x and y, Δx and Δy, respectively, can vary spatially and must be stored as two-dimensional (2-D) arrays, (2) the fluxes between grid cells must account for the changing size of the grid cells, and (3) correction terms are needed to account for the exchange between u and v momentum due to horizontal transport along curving grid coordinates.

The spatial finite differencing in NCOM is done in conservative form with the advective and diffusive transport between grid cells calculated as fluxes between the grid cells. The use of this form maintains conservation of the scalar model fields for transport between grid cells regardless of how the size of the grid cells change.

With transport conservation satisfied by the flux form used for differencing, the main remaining requirement for the use of a curvilinear grid is that, since the horizontal velocity components u and v follow (i.e., are directed along) curving horizontal coordinates, there is, in effect, a conversion of momentum between the two horizontal velocity components as momentum is transported along a curving grid coordinate. There is a correction for both the horizontal advection and diffusion terms to account for interchange between u and v momentum on a curvilinear grid. POM does not provide a curvature correction for the horizontal diffusion terms in the momentum equations and none is currently provided in NCOM. The assumption is that the transport of momentum due to horizontal diffusion is sufficiently small that error due to neglect of the curvature correction to this term will not be significant.

To keep truncation errors associated with curvilinear grids relatively small, a rule of thumb in using such grids is to not change the size of the grid spacing by more than about 10% between successive grid cells. With the simple two-point averages and differences used for the finite differencing, the accuracy of spatial interpolations and gradients becomes first-order rather than second-order if the change in size between successive grid cells becomes more than a small fraction of the grid spacing.

The philosophy that has been followed to date in applying NCOM has been to avoid using grid curvature, except as needed to adapt the model grid to large-scale map projections where the

grid curvature is very gradual, to minimize spatial truncation errors. In our coastal simulations to date, we have not encountered a need to use strong grid curvature. The entire grid can be rotated to provide a desired orientation along a section of coastline, and shrinkwrapping can be used to eliminate calculations over land areas along the sides of the domain. Most coastlines are so irregular that curvilinear coordinates cannot be curved sufficiently to follow them with any fidelity.

Figure 1 shows the horizontal arrangement of some of the variables on the model grid. The horizontal arrangement of the variables uses the form of the Arakawa C grid. With the C grid, scalar fields such as T, S, and ρ are located at the grid-cell midpoints, and each of the velocity components is located at the center of the grid-cell face to which it is normal.

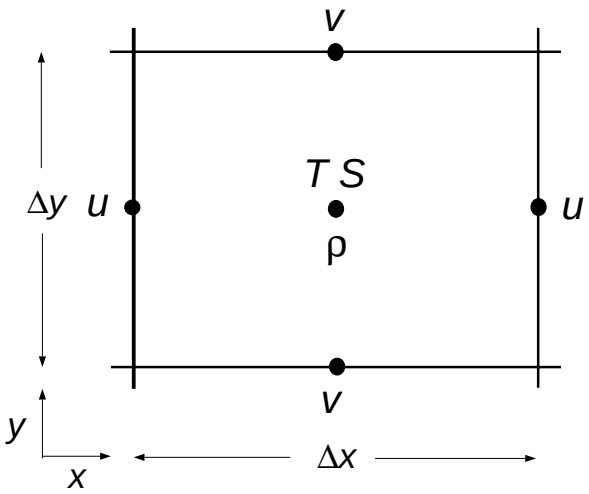

Fig. 1 — Horizontal layout of variables on model grid

3.2 Vertical Grid

The model uses a combined sigma/z-level vertical grid with sigma layers near the surface and z-levels below a depth that can be specified by the user.

Figure 2 illustrates the different ways the combined sigma/z-level vertical grid can be set up. Figure 2(a) shows the vertical grid set up with a single sigma layer at the surface and with z-levels below. Since the model has a free surface, at least one sigma layer is needed at the surface to allow for changes in the surface elevation.

If the changes in the surface elevation are large relative to the grid resolution desired near the surface, a single sigma layer may not be sufficient to resolve the changes in the surface elevation. In this case, several sigma layers can used, and the changes in the surface elevation will be distributed among them (Fig. 2(b)).

If the water depth becomes shallower than the depth that defines the transition from sigma layers to z-levels (z_σ), the sigma layers will shallow uniformly as the bottom depth decreases. Figure 2(c) shows a grid in which the sigma layers extend to the bottom in the shallow water on the shelf, and z-levels are used in the deeper water off the shelf. Figure 2(d) shows a grid in which sigma layers are used all the way to the bottom everywhere.

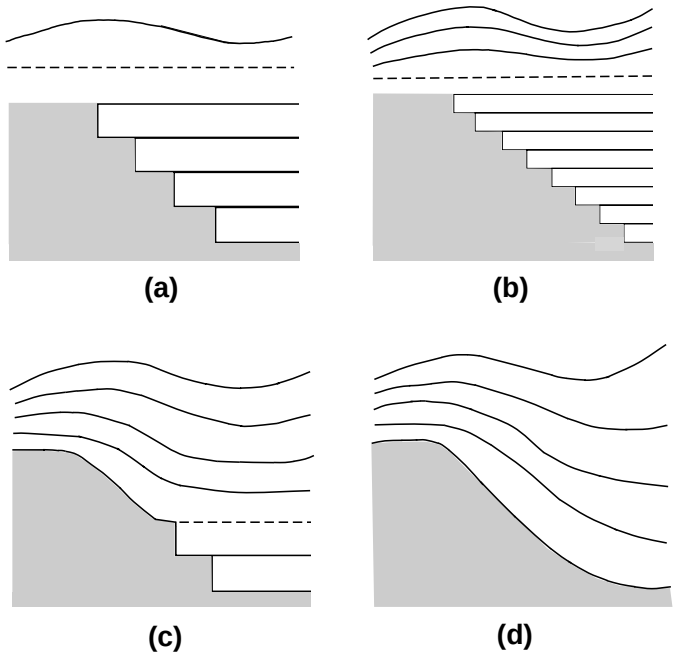

Fig. 2 — Illustration of the different ways the combined sigma/z-level grid can be set up: (a) with a single sigma layer at the surface, (b) with several sigma layers at the surface to resolve surface elevation changes, (c) with sigma layers in the shallow water and z-levels in the deep water, and (d) with sigma layers all the way to the bottom everywhere

Figure 3 shows the vertical arrangement of some of the model variables on the model grid. As in the layout of the horizontal grid, the main scalar fields are located at grid-cell centers, and the velocity components are located at the center of the grid-cell face to which they are normal.

The coordinate transformation for the sigma coordinate part of the grid is given by

$$\sigma = \frac{z - \zeta}{D_\sigma}, \tag{70}$$

where $D_\sigma = \zeta - \max(H, z_\sigma)$. Hence, σ varies from $\sigma = 0$ at the free surface to $\sigma = -1$ at the bottom interface of the lowest sigma layer. Each sigma layer is a fixed fraction of the total depth of the sigma grid D_σ.

Similar to the implementation of orthogonal, curvilinear coordinates, the implementation of sigma coordinates is primarily a matter of accounting for the changing vertical thickness of the layers in calculating fluxes between adjacent grid cells and in calculating changes within the grid cells. Note that with sigma coordinates, the changes in the thickness of the grid cells occurs not only horizontally within a layer but also from timestep to timestep because of the changing surface elevation. To avoid having to use a large number of 3-D arrays to store the thickness of the grid cells at different locations and time levels, the grid thickness Δz for a sigma layer is expressed as the product of the fractional thickness of the sigma layer $\Delta\sigma$ times the depth from the surface to the bottom of the sigma coordinate grid, i.e., as

$$\Delta z = \Delta\sigma D_\sigma. \tag{71}$$

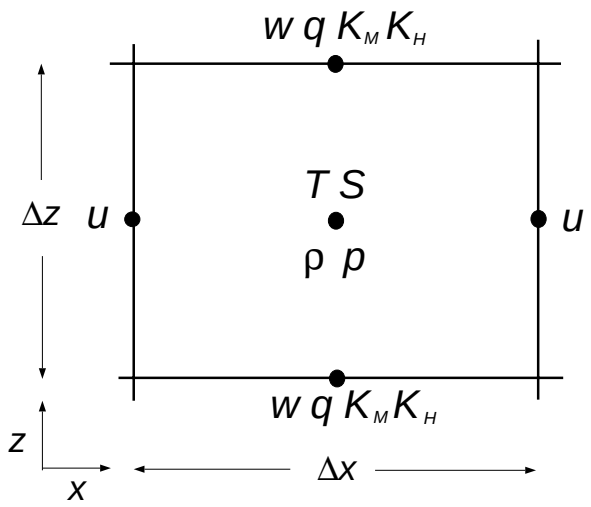

Fig. 3 — Vertical layout of variables on model grid

The vertical velocity on the sigma coordinate grid ω is the vertical velocity relative to the sigma surfaces. This velocity is not the true vertical velocity since it is missing the vertical component of the flow along the sigma layers (if they are sloping) as well as the vertical velocity due to the vertical motion of the sigma surfaces themselves caused by the rise and fall of the sea surface. The velocity ω is related to the Cartesian vertical velocity w as

$$w = \omega + (1-\sigma)\frac{\partial \zeta}{\partial t} + u\frac{\partial}{\partial x}(\zeta + \sigma D_\sigma) + v\frac{\partial}{\partial y}(\zeta + \sigma D_\sigma). \tag{72}$$

Since the surfaces on the z-level grid are level and fixed in time, $w = \omega$ on the z-level grid.

The form of the model equations in sigma coordinates is presented in Appendix B. The only significant modification to the basic equations for the changing depth of the sigma layers, with regard to converting the equations to finite difference form, is a correction for the horizontal pressure gradient. The horizontal pressure gradient calculation in sigma coordinates contains an extra term to remove the vertical change in pressure between neighboring points within a sigma layer, so that the net pressure change that is computed will be approximately along a level surface (Blumberg and Mellor 1987). The form of the horizontal pressure gradient in sigma coordinates is modified from the Cartesian form (Eq. (20)) used on the z-level part of the grid to

$$\frac{1}{\rho_o}\frac{\partial p}{\partial x} = \frac{1}{\rho_o}\frac{\partial p(\zeta)}{\partial x} + g\frac{\partial \zeta}{\partial x} + \frac{gD_\sigma}{\rho_o}\int_\sigma^0 \left[\frac{\partial \rho}{\partial x}|_\sigma - \frac{\sigma}{D_\sigma}\frac{\partial D_\sigma}{\partial x}\frac{\partial \rho}{\partial \sigma}\right] d\sigma, \tag{73}$$

where the term $\frac{\partial \rho}{\partial x}|_\sigma$ is the density gradient taken along a surface of constant σ.

A potential problem with this calculation of the pressure gradient in sigma coordinates is that the vertical component of the pressure change along a sloping sigma surface is frequently much larger than the horizontal component along a level surface (Haney 1991). In this case, the desired horizontal component is calculated as the small difference between two large terms and is subject to significant truncation error. An expedient that is commonly used to reduce this error is to subtract the horizontally averaged density profile from the 3-D density field when calculating the horizontal

pressure gradient, so that the main component of the vertical change in pressure is removed from the calculation, i.e., ρ in Eq. (73) is replaced by $\rho - \overline{\rho}(z)$, where $\overline{\rho}(z)$ is the horizontal mean density profile (Blumberg and Mellor 1987).

Strictly speaking, for a full transformation of the equations to sigma coordinates, the horizontal diffusion terms should be corrected for the transformation, so that they will still represent diffusion along level surfaces. However, NCOM (and POM) use the approximation discussed by Mellor and Blumberg (1985), who argued that diffusion along the sigma surfaces rather than along level surfaces was, in general, more appropriate for sigma coordinate models, particularly for proper simulation of the bottom boundary layer.

However, in regions where there are large changes in the bottom depth, the horizontal diffusion along sloping sigma layers can cause severe cross-isopycnal diffusion (Paul 1994). An expedient that is sometimes used with sigma coordinate models (Mellor and Blumberg 1985), and is an option in NCOM, is to subtract a smooth background field from the T or S fields when calculating horizontal diffusion. By calculating the horizontal diffusion based on the anomaly from a smooth background field, most of the component of vertical diffusion that occurs when diffusion is calculated along sloping sigma layers is eliminated.

In domains where the T and S fields don't vary much, the background T and S fields can be calculated as the horizontally averaged T and S profiles. An alternative strategy is to use smooth but horizontally varying background fields to accommodate changes in the structure of the T and S fields in different parts of the model domain. The background fields can also be periodically updated to accommodate changes in T and S that occur in time. The use of these procedures can significantly reduce the problem of severe cross-isopycnal diffusion (however, as discussed in Section 4.2, they can introduce other problems).

On the z-level part of the grid, the bathymetry is rounded to the nearest z-level. This is the simplest way to implement bathymetry in a z-level model and is the way the bathymetry has been incorporated into a number of ocean models, including the various versions of the Bryan-Cox model (Bryan 1969; Killworth et al. 1991; Dukowicz and Smith 1994), the Haney model (Haney 1974), and the DieCAST model (Dietrich and Ko 1994). There are, however, a number of limitations to this representation of the bathymetry, which are discussed in Section 4.3.

3.3 Spatial Differencing

Spatial interpolations and gradients use second-order centered averages and differences. With second-order, centered interpolations, the value of a variable ϕ at a location between points at which the variable is defined is evaluated as the average of the values on either side, e.g., for an interpolation in the x direction,

$$\overline{\phi}^{x} = \frac{1}{2}(\phi_{x+\Delta x/2} + \phi_{x-\Delta x/2}). \tag{74}$$

With second-order, centered differencing, the gradient of ϕ at x is calculated as the difference of the values on either side

$$\frac{\partial \phi}{\partial x}|_{x} = \frac{1}{\Delta x}\delta_{x}\phi = \frac{1}{\Delta x}(\phi_{x+\Delta x/2} - \phi_{x-\Delta x/2}). \tag{75}$$

3.4 Temporal Differencing

The leapfrog scheme is used for temporal differencing. The temporal differencing of the 3-D equations will be illustrated here with just the u momentum equation since the treatment of the other model variables is similar. In the following discussion, n will denote model values at the current time level (i.e., values calculated on the previous timestep), $n+1$ will denote the newly calculated values, and $n-1$ will denote values at the previous time level.

With the leapfrog scheme, most of the terms (i.e., the advection, baroclinic pressure gradient, and Coriolis terms) are centered in time at n. The horizontal diffusion terms are evaluated at the $n-1$ time level for the variable being diffused (since evaluation of the variable being diffused at the central time level of a leapfrog scheme is numerically unstable), and the vertical diffusion terms are treated implicitly so as to avoid the timestep restriction for explicit vertical diffusion (the high rates of vertical diffusion that are frequently calculated by the turbulence schemes would require a very small timestep for stability if the vertical diffusion were explicit). Hence, the temporal differencing of the u momentum equation is of the form

$$\frac{\delta_{2t}u}{2\Delta t} = \frac{u^{n+1}-u^{n-1}}{2\Delta t} = -\nabla\cdot(\mathbf{v}u)^n + fv^n - \frac{1}{\rho_o}\frac{\partial p^n}{\partial x} + F_u^{n-1} + \frac{\partial}{\partial z}\left(K_M\frac{\partial u^{n+1}}{\partial z}\right). \tag{76}$$

An Asselin filter is used to suppress the time splitting that can occur with leapfrog (Asselin 1972). The Asselin filter is applied to the model fields at time level n, after the new values at $n+1$ have been calculated, by averaging in a bit of the values at the $n+1$ and $n-1$ time levels, i.e.,

$$\phi^n = \nu(\phi^{n+1}+\phi^{n-1}) + (1-2\nu)\phi^n, \tag{77}$$

where ν is the filter coefficient. If Eq. (77) is rewritten as

$$\phi^n = \phi^n + \nu(\phi^{n+1} - 2\phi^n + \phi^{n-1}), \tag{78}$$

the filter looks like a numerical diffusion term, which is the way that it behaves. A typical value used for ν is 0.05.

3.5 Finite Difference Form of the Model Equations

As noted earlier, the model equations are finite differenced in flux-conservative form. The full finite difference form of the basic 3-D model equations used in NCOM is

$$\begin{aligned}\frac{\Delta x^u\Delta y^u}{2\Delta t}\delta_{2t}(\Delta z^u u) = &-\Delta y^u\Delta z^u g\delta_x(\zeta^* + \zeta_{atm} - \zeta_{tp}) - \Delta y^u\Delta z^u\frac{1}{\rho_o}\delta_x(p_i)\\ &+ \overline{\Delta x\Delta y\Delta z(f+C_{curv})\overline{v}^y}^x\\ &- \delta_x(\overline{\Delta y^u\Delta z^u u^a}^x\overline{u}^x) - \delta_y(\overline{\Delta x^v\Delta z^v v^a}^x\overline{u}^y)\\ &- \delta_z(\overline{\Delta x\Delta y\omega}^x\overline{u}^z) + \overline{\Delta x\Delta y\Delta z Q}^x u_{sor} + F_u^*\\ &+ \Delta x^u\Delta y^u\delta_z\left(\frac{\overline{K_M}^x}{(\overline{\Delta z^{w}}^x)^{n+1}}\delta_z u^{n+1}\right)\end{aligned} \tag{79}$$

$$\frac{\Delta x^v \Delta y^v}{2\Delta t}\delta_{2t}(\Delta z^v v) = -\Delta x^v \Delta z^v g \delta_y(\zeta^* + \zeta_{atm} - \zeta_{tp}) - \Delta x^v \Delta z^v \frac{1}{\rho_o}\delta_y(p_i)$$
$$- \overline{\Delta x \Delta y \Delta z (f + C_{curv}) \overline{u}^x}^y$$
$$- \delta_x(\overline{\Delta y^u \Delta z^u u^a}^y \overline{v}^x) - \delta_y(\overline{\Delta x^v \Delta z^v v^a}^x \overline{v}^y)$$
$$- \delta_z(\overline{\Delta x \Delta y \omega}^y \overline{v}^z) + \overline{\Delta x \Delta y \Delta z Q}^y v_{sor} + F_v^*$$
$$+ \Delta x^v \Delta y^v \delta_z \left(\frac{\overline{K_M}^y}{(\overline{\Delta z^w}^y)^{n+1}} \delta_z v^{n+1} \right) \tag{80}$$

$$\frac{\Delta x \Delta y}{2\Delta t}\delta_{2t}(\Delta z) = -\delta_x(\Delta y^u \Delta z^u u^a) + -\delta_y(\Delta x^v \Delta z^v v^a) + -\delta_z(\Delta x \Delta y \omega)$$
$$+ \Delta x \Delta y \Delta z Q \tag{81}$$

$$\frac{\Delta x \Delta y}{2\Delta t}\delta_{2t}(\Delta z T) = -\delta_x(\Delta y^u \Delta z^u u^a \overline{T}^x) - \delta_y(\Delta x^v \Delta z^v v^a \overline{T}^y)$$
$$- \delta_z(\Delta x \Delta y \omega \overline{T}^z) + \Delta x \Delta y \Delta z Q T_{sor}$$
$$+ \delta_x \left(\frac{\Delta y^u \Delta z^u A_H^u}{\Delta x^u} \delta_x T^{n-1} \right) + \delta_y \left(\frac{\Delta x^v \Delta z^v A_H^v}{\Delta y^v} \delta_y T^{n-1} \right)$$
$$+ \Delta x \Delta y \delta_z \left(\frac{K_H}{(\Delta z^w)^{n+1}} \delta_z T^{n+1} \right) + \Delta x \Delta y Q_r \delta_z \gamma \tag{82}$$

$$\frac{\Delta x \Delta y}{2\Delta t}\delta_{2t}(\Delta z S) = -\delta_x(\Delta y^u \Delta z^u u^a \overline{S}^x) - \delta_y(\Delta x^v \Delta z^v v^a \overline{S}^y)$$
$$- \delta_z(\Delta x \Delta y \omega \overline{S}^z) + \Delta x \Delta y \Delta z Q S_{sor}$$
$$+ \delta_x \left(\frac{\Delta y^u \Delta z^u A_H^u}{\Delta x^u} \delta_x S^{n-1} \right) + \delta_y \left(\frac{\Delta x^v \Delta z^v A_H^v}{\Delta y^v} \delta_y S^{n-1} \right)$$
$$+ \Delta x \Delta y \delta_z \left(\frac{K_H}{(\Delta z^w)^{n+1}} \delta_z S^{n+1} \right), \tag{83}$$

where ζ_{atm} is the atmospheric surface pressure (expressed in meters of water), ζ_{tp} is the tidal potential, p_i is the internal (baroclinic) pressure, u^a and v^a are the horizontal advection velocities, and F_u^* and F_v^* are the finite difference forms of the horizontal momentum mixing terms. The variables are evaluated at time level n unless otherwise noted. Note that the temporal changes in the height of the grid cells Δz that occur on the sigma coordinate part of the grid are accounted for in the finite difference equations.

The primary grid-cell dimensions Δx, Δy, and Δz are defined at the center of the grid cells. The superscripts u, v, and w denote grid-cell dimensions at the u, v, and w velocity locations, respectively. These are obtained by averaging the grid-cell dimensions of the adjoining grid cells (e.g., $\Delta x^u = \overline{\Delta x}^x$).

The evaluation of the surface elevation term ζ^* can be distributed among any of the three time levels, i.e.,

$$\zeta^* = \alpha_1 \zeta^{n+1} + \alpha_2 \zeta^n + \alpha_3 \zeta^{n-1}, \tag{84}$$

where the temporal weights α_1, α_2, and α_3 are specified by the user (see Section 3.6).

The variable C_{curv} in Eqs. (79) and (80) is used to correct the horizontal momentum advection for the horizontal curvature of the grid. The curvature correction term for advection has a form similar to that of the Coriolis term (Appendix A). C_{curv} is calculated as

$$C_{curv} = \overline{v}^{y} \frac{\delta_{2x}(\Delta y)}{2\Delta x \Delta y} - \overline{u}^{x} \frac{\delta_{2y}(\Delta x)}{2\Delta x \Delta y}. \tag{85}$$

On the sigma coordinate part of the grid, an option is provided to calculate the horizontal diffusion of scalar fields relative to a spatially smooth mean or climatological field. In this case, T^* and S^* in the horizontal diffusion terms are set equal to $T - T_{mean}$ and $S - S_{mean}$, respectively, where T_{mean} and S_{mean} are mean or climatological or horizontally averaged fields. On the z-level grid and on the sigma coordinate grid, if this option is not used, $T^* = T$ and $S^* = S$.

3.6 Calculation of the Free-Surface Mode

The free-surface mode is calculated implicitly. Hence, the surface pressure gradients and the divergence terms in the surface elevation equation have a component at the new time level being calculated. The finite difference equations for the free-surface mode are

$$\frac{\Delta x^u \Delta y^u}{2\Delta t} \delta_{2t}(D^u \overline{u}) = -\Delta y^u D^u g \delta_x(\alpha_1 \zeta^{n+1} + \alpha_2 \zeta^n + \alpha_3 \zeta^{n-1}) + D^u \overline{G_u}, \tag{86}$$

$$\frac{\Delta x^v \Delta y^v}{2\Delta t} \delta_{2t}(D^v \overline{v}) = -\Delta x^v D^v g \delta_y(\alpha_1 \zeta^{n+1} + \alpha_2 \zeta^n + \alpha_3 \zeta^{n-1}) + D^v \overline{G_v}, \tag{87}$$

$$\begin{aligned} \frac{\Delta x \Delta y}{2\Delta t} \delta_{2t} \zeta = & -\delta_x(\Delta y^u(\beta_1(D^u \overline{u})^{n+1} + \beta_2(D^u \overline{u})^n + \beta_3(D^u \overline{u})^{n-1})) \\ & - \delta_y(\Delta x^v(\beta_1(D^v \overline{v})^{n+1} + \beta_2(D^v \overline{v})^n + \beta_3(D^v \overline{v})^{n-1})) + \Delta x \Delta y D \overline{Q}, \end{aligned} \tag{88}$$

where $D^u \overline{G_u}$ and $D^v \overline{G_v}$ are the vertical integrals of all the terms on the left side of Eqs. (79) and (80), respectively, except for the surface elevation gradient terms, and $D^u = \overline{D}^x$ and $D^v = \overline{D}^y$.

The variables α_1, α_2, and α_3 are constants that specify the fractional weighting of the surface elevation gradient in the momentum equations at the new, current, and previous time levels. Similarly, β_1, β_2, and β_3 specify the fractional weighting of the divergence terms in the depth-averaged continuity equation at the new, current, and previous time levels. These weightings can be set by the user. Commonly used values are $\alpha_1 = \alpha_3 = \beta_1 = \beta_3 = 0.5$ and $\alpha_2 = \beta_2 = 0$ (see Section 4.4).

The equations for the free-surface mode are solved by substituting the expressions for $(D^u \overline{u})^{n+1}$ and $(D^v \overline{v})^{n+1}$ from Eqs. (86) and (87) into Eq. (88) and solving for the new surface elevation ζ^{n+1}. The resulting equation is an elliptic equation for ζ^{n+1}, which can be solved with an iterative or a direct method (NCOM currently uses an iterative solver).

3.7 Baroclinic Pressure Gradient

On the sigma coordinate part of the grid, the baroclinic pressure gradient is calculated for a particular layer k as

$$\frac{1}{\rho_o}\delta_x p_i|_k = \frac{1}{\rho_o}\delta_x p_i|_{k-1} + \frac{g}{\rho_o}(\frac{1}{4}D^u(\Delta\sigma_{k-1}+\Delta\sigma_k)\delta_x(\rho^*_{k-1}+\rho^*_k) - \frac{1}{2}(\sigma_{k-1}+\sigma_k)(\delta_x D)(\delta_\sigma\overline{\rho^*}^x)), \tag{89}$$

and on the z-level part of the grid, the baroclinic pressure gradient is calculated as

$$\frac{1}{\rho_o}\delta_x p_i|_k = \frac{1}{\rho_o}\delta_x p_i|_{k-1} + \frac{g}{\rho_o}\frac{1}{2}(\Delta z_{k-1}\delta_x\rho_{k-1} + \Delta z_k\delta_x\rho_k), \tag{90}$$

where $\rho^* = \rho - \overline{\rho}(z)$, and $\overline{\rho}(z)$ is the horizontally averaged density.

3.8 Horizontal Advection

The advection velocities u^a and v^a in Eqs. (79) to (83) are calculated from u^n and v^n, respectively, but the vertical means of u^a and v^a are adjusted to match the mean vertical velocity needed to account for the change in the surface elevation between time levels $n-1$ and $n+1$. Hence,

$$u^a = u^n + \beta_1\overline{u}^{n+1} + \beta_2\overline{u}^n + \beta_3\overline{u}^{n-1} - \overline{u}^n \tag{91}$$

$$v^a = v^n + \beta_1\overline{v}^{n+1} + \beta_2\overline{v}^n + \beta_3\overline{v}^{n-1} - \overline{v}^n. \tag{92}$$

The purpose of this adjustment is to ensure that the advection velocity field satisfies continuity exactly for advection of the scalar fields.

3.9 Horizontal Mixing

For the grid-cell Reynolds number calculation of the horizontal mixing, the horizontal mixing coefficients are calculated at the staggered velocity points as

$$A^u_M = \max\left[A_o, \frac{|u^n|\Delta x^u}{R_{e_g}}\right] \tag{93}$$

$$A^v_M = \max\left[A_o, \frac{|v^n|\Delta y^v}{R_{e_g}}\right], \tag{94}$$

and the finite difference form of the mixing terms for the momentum equations is

$$F^*_u = \delta_x(\overline{\Delta y^u\Delta z^u A^u_M/\Delta x^u}^x\delta_x u^{n-1}) + \delta_y(\overline{\Delta x^v\Delta z^v A^v_M/\Delta y^v}^x\delta_y u^{n-1}), \tag{95}$$

$$F^*_v = \delta_x(\overline{\Delta y^u\Delta z^u A^u_M/\Delta x^u}^y\delta_x v^{n-1}) + \delta_y(\overline{\Delta x^v\Delta z^v A^v_M/\Delta y^v}^y\delta_y v^{n-1}). \tag{96}$$

For the Smagorinsky horizontal mixing, the horizontal mixing coefficients are calculated at the grid-cell centers as

$$A_M = C_{smag}\Delta x\Delta y\left[\left(\frac{1}{\Delta x}\delta_x u^n\right)^2 + \frac{1}{2}\left(\frac{1}{2\Delta y}\delta_{2y}\overline{u^n}^x + \frac{1}{2\Delta x}\delta_{2x}\overline{v^n}^y\right)^2 + \left(\frac{1}{\Delta y}\delta_y v^n\right)^2\right]^{\frac{1}{2}}. \tag{97}$$

If the mixing coefficients are then averaged to the staggered velocity points,

$$A_M^u = \overline{A_M}^x, \tag{98}$$

$$A_M^v = \overline{A_M}^y. \tag{99}$$

The finite difference form of the mixing terms for the momentum equations used for the Smagorinsky scheme is

$$\begin{aligned} F_u^* = {} & \delta_x(2\overline{\Delta y^u \Delta z^u A_M^u/\Delta x^u}^x \delta_x u^{n-1}) \\ & + \delta_y(\overline{\Delta x^v \Delta z^v A_M^v/\Delta y^v}^x \delta_y u^{n-1} + \overline{\Delta x^v \Delta z^v A_M^v/\Delta x^v}^x \delta_x v^{n-1}), \end{aligned} \tag{100}$$

$$\begin{aligned} F_v^* = {} & \delta_x(\overline{\Delta y^u \Delta z^u A_M^u/\Delta y^u}^y \delta_y u^{n-1} + \overline{\Delta y^u \Delta z^u A_M^u/\Delta x^u}^y \delta_x v^{n-1}) \\ & + \delta_y(2\overline{\Delta x^v \Delta z^v A_M^v/\Delta y^v}^y \delta_y v^{n-1}). \end{aligned} \tag{101}$$

3.10 Vertical Mixing

Vertical mixing is fully implicit, e.g., the vertical heat flux is computed as

$$-K_H \frac{\partial T^{n+1}}{\partial z}. \tag{102}$$

Fully implicit vertical mixing is needed to avoid spurious flip-flopping of the vertical gradients, which can occur with a partially implicit scheme when the vertical eddy coefficients become very large in regions of strong vertical mixing. The implicit treatment of vertical mixing couples the 3-D prognostic equations in the vertical and requires the use of a tridiagonal solver at each horizontal point to solve for the new values.

The finite difference form for the prognostic equations for the MYL2.5 turbulence scheme (Eqs. (32) and (33)) is

$$\begin{aligned} \frac{\Delta x \Delta y}{2\Delta t}\delta_{2t}(\Delta z^w q^2) = {} & -\delta_x(\overline{\Delta y^u \Delta z^u u^a}^z \overline{q^2}^x) - \delta_y(\overline{\Delta x^v \Delta z^v v^a}^z \overline{q^2}^y) \\ & - \delta_z(\overline{\Delta x \Delta y \omega}^z \overline{q^2}^z) + \overline{\Delta x \Delta y \Delta z Q}^z q_{sor}^2 \\ & + \delta_x\left(\overline{\frac{\Delta y^u \Delta z^u A_H^u}{\Delta x^u}}^z \delta_x (q^2)^{n-1}\right) + \delta_y\left(\overline{\frac{\Delta x^v \Delta z^v A_H^v}{\Delta y^v}}^z \delta_v (q^2)^{n-1}\right) \\ & + \Delta x \Delta y \delta_z\left(\frac{\overline{K_{q_1}}^z}{(\Delta z)^{n+1}} \delta_z q^{2^{n+1}}\right) \\ & + \Delta x \Delta y \Delta z^w (2K_{M_1}\left(\left(\frac{\delta_z u}{\Delta z^w}\right)^2 + \left(\frac{\delta_z v}{\Delta z^w}\right)^2\right) + \\ & 2K_{H_1}\left(\frac{g\delta_z \tilde{\rho}}{\rho_o \Delta z^w}\right) - \frac{2(q^2)^{n+1} q^{n-1}}{b_1 \ell^{n-1}}), \end{aligned} \tag{103}$$

$$\frac{\Delta x\Delta y}{2\Delta t}\delta_{2t}(\Delta z^w q^2\ell) = -\delta_x(\overline{\Delta y^u\Delta z^u u^a}^z\overline{q^2\ell}^x) - \delta_y(\overline{\Delta x^v\Delta z^v v^a}^z\overline{q^2\ell}^y)$$
$$- \delta_z(\overline{\Delta x\Delta y\omega}^z\overline{q^2\ell}^z) + \overline{\Delta x\Delta y\Delta z Q}^z(q^2\ell)_{sor}$$
$$+ \delta_x\left(\frac{\overline{\Delta y^u\Delta z^u A_H^u}^z}{\Delta x^u}\,\delta_x(q^2\ell)^{n-1}\right) + \delta_y\left(\frac{\overline{\Delta x^v\Delta z^v A_H^v}^z}{\Delta y^v}\,\delta_v(q^2\ell)^{n-1}\right)$$
$$+ \Delta x\Delta y\delta_z\left(\frac{\overline{K_{q_1}}^z}{(\Delta z)^{n+1}}\delta_z(q^2\ell)^{n+1}\right)$$
$$+ \Delta x\Delta y\Delta z^w(E_1\ell(K_{M_1}\left(\left(\frac{\delta_z u}{\Delta z^w}\right)^2 + \left(\frac{\delta_z v}{\Delta z^w}\right)^2\right) +$$
$$E_3 K_{H_1}\left(\frac{g\delta_z\tilde{\rho}}{\rho_o\Delta z^w}\right)) - \frac{2(q^2)^{n+1}q^{n-1}}{b_1\ell^{n-1}}W). \tag{104}$$

The variables are at time level n unless otherwise noted. The new values of K_{M_1} and K_{H_1} for the MYL2.5 scheme are then calculated as

$$K_{M_1} = (\ell^{n+1}q^{n+1}S_M + K_{M_1}^{old})/2, \tag{105}$$

$$K_{H_1} = (\ell^{n+1}q^{n+1}S_H + K_{H_1}^{old})/2, \tag{106}$$

where $K_{M_1}^{old}$ and $K_{H_1}^{old}$ are the values of K_{M_1} and K_{H_1} calculated on the previous timestep. The purpose of averaging with values calculated on the previous timestep is to provide a strong temporal smoothing of K_{M_1} and K_{H_1}. Without this type of averaging, the vertical eddy coefficients tend to be noisy. S_M and S_H are calculated from G_H using Eqs. (42) and (43) where

$$G_H = \min\left[0.028, \left(\frac{\ell^{n+1}}{q^{n+1}}\right)^2\frac{g}{\rho_o}\frac{\partial\tilde{\rho}^n}{\partial z}\right]. \tag{107}$$

Note that the eddy coefficients calculated with the MYL2.5 scheme in NCOM are not applied until the next timestep (Section 3.12). Since the values of momentum and density used to calculate the new values of K_{M_1} and K_{H_1} for the MYL2.5 scheme are at time level n and the new values of K_{M_1} and K_{H_1} are applied at the next timestep, the vertical eddy coefficients are calculated from the same leapfrog solution (i.e., odd or even) to which they are applied, which helps to suppress timesplitting.

For the MYL2 scheme, S_M, S_H, and q are calculated using Eqs. (50) to (64) with the values of momentum and density at time level $n-1$. For the MYL2 scheme in NCOM, the new values of K_{M_1} and K_{H_1} are applied on the same timestep at which they are calculated (Section 3.12). Hence, as for the MYL2.5 scheme, K_{M_1} and K_{H_1} are calculated from the same leapfrog solution to which they are applied. Also as for the MYL2.5 scheme, the new values of K_{M_1} and K_{H_1} are averaged with the previously calculated values to reduce noise.

3.11 Bottom Drag

The bottom drag is partially implicit to improve stability and is calculated as

$$K_M \frac{\partial u}{\partial z} = c_b u^{n+1} \mid \mathbf{v}^{n-1} \mid \tag{108}$$

and

$$K_M \frac{\partial v}{\partial z} = c_b v^{n+1} \mid \mathbf{v}^{n-1} \mid . \tag{109}$$

The explicit part of the bottom drag terms is at the old time level $n-1$ to avoid exciting time-splitting.

3.12 Calculation Sequence

The calculation sequence for the model is as follows:

(1) Advection velocities and horizontal eddy coefficients needed for momentum, new densities, and new baroclinic pressure gradients are calculated. If the MYL2 turbulence scheme is being used, new vertical eddy coefficients are calculated.

(2) New 3-D horizontal velocities are calculated and the forcing terms from the 3-D momentum equations are vertically integrated to provide the forcing terms needed for the depth-averaged momentum equations that are used to calculate the free-surface mode.

(3) The depth-averaged momentum and continuity equations are solved for the new surface elevation and depth-averaged velocities.

(4) The new 3-D velocity fields calculated in Step 2 are corrected by adding a depth-independent adjustment, so that their vertical mean agrees with the new depth-averaged velocities calculated in Step 3. This effectively corrects the 3-D velocities for the new surface elevation gradient.

(5) The velocity field that will be used to advect the scalar fields is calculated by adding a depth-independent adjustment to the 3-D velocity fields at time level n, so that the depth-averaged advection velocities are consistent with the depth-averaged continuity equation.

(6) New values of the scalar fields (T and S) are calculated using the advection fields computed in Step 4. If the MYL2.5 turbulence scheme is being used, the turbulence fields are updated and new vertical eddy coefficients are calculated. These fields are Asselin-filtered as the new values are calculated.

(7) An Asselin filter is applied to the velocity and surface elevation fields. The filtered 3-D velocities are then corrected to be consistent with the filtered depth-averaged velocities using the same procedure as in Step 4.

The adjustment of the advection velocities in Step 5 ensures that the velocity field used to advect the scalar fields is numerically nondivergent. This is necessary to avoid spurious sources and sinks when using the flux form of numerical advection.

It is desirable that the velocity field used for advection of momentum also be nondivergent and consistent with the change in surface elevation. However, when the 3-D momentum equations

and the forcing for the free-surface mode are calculated in Step 2, the new surface elevation is not yet known. Hence, it is not possible for the momentum advection and the change in elevation to be fully consistent without some sort of iterative process. This is also a problem for free-surface models such as POM that use a separate, small timestep (i.e., the split-explicit scheme) for the free-surface equations. Iteration of the solution of the 3-D momentum and continuity equations and the depth-averaged equations (Steps 1 to 5 above) to eliminate this inconsistency is provided for in NCOM. However, in tests that have been conducted to date, the effect of iterating to remove the slight inconsistency between the momentum advection and the change in surface elevation was not significant.

Another difficulty in the numerical calculation involves the partially implicit bottom drag term. If the bottom drag were treated explicitly, the implicit vertical mixing and the bottom drag calculation would be numerically decoupled from the solution of the depth-averaged equations. However, when the bottom drag calculation involves the new velocities, the bottom drag calculation and the solution of the depth-averaged equations are not decoupled. The initial, uncorrected estimate of the new 3-D velocities will be involved in the calculation of the bottom drag, which is part of the forcing term for the free-surface mode. This is another reason why it is important that the initial calculation of the new 3-D velocities (i.e., uncorrected for the new surface elevation) in Step 2 be as accurate as possible. Currently, in the initial calculation of the 3-D velocities, the new surface elevation is estimated from the horizontal divergence of the velocity field at time level n.

3.13 Shrinkwrapping and Slicing

The model calculations are shrinkwrapped in the x-direction to avoid calculating over land areas on the sides of the domain. What this means is that the calculations start at the first sea point and end at the last sea point along each row of grid cells in the x-direction. How successful this procedure is in reducing calculations depends on the particular distribution of land and sea areas in the model domain. For many coastal problems, shrinkwrapping can provide a useful increase in model performance.

Slicing is the procedure of calculating through the model domain in x-z slices and performing as many calculations as possible on each x-z slice before moving on to the next one. The purpose of this is to reuse variables that have already been brought into high-speed cache memory to avoid the slower accesses from main memory. If each calculation in the code is performed over the entire domain, variables are more likely to be flushed out of high-speed cache before they are reused. Each timestep of the model requires two major passes through the model domain, one to update the momentum fields and another to update the scalar fields. How much the x-z slicing improves program speed depends on the relative size of the domain and the particular computer being used.

4. MODEL LIMITATIONS

When using a model, it is important to be aware of its limitations. The purpose of this section is to discuss some of the limitations of the physical and numerical parameterizations in NCOM.

4.1 Hydrostatic Approximation

Like most ocean models, NCOM uses the hydrostatic assumption in which the vertical momentum equation is reduced to a balance between the gravitational acceleration and vertical pressure

gradient terms (Eq. (3)). In particular, the vertical acceleration terms are ignored. This is a fairly good assumption for large-scale oceanic flows where the vertical acceleration terms are usually fairly small relative to the hydrostatic terms. The assumption is less valid at small scales where vertical acceleration terms become relatively more important.

Casulli and Stelling (1996) illustrate some situations where the hydrostatic assumption breaks down. One example is that of a propagating freshwater plume. As the plume advances into the ambient fluid, there is a convergence near the surface at the front of the plume where the water is accelerated downward and underneath the advancing plume. If such a plume is modeled with a hydrostatic model, one finds that as the horizontal grid resolution is increased, the downward velocity at the front of the plume continues to increase to values that are significantly higher than the correct values. This is because the vertical velocity in the hydrostatic model is calculated strictly from the divergence of the horizontal flow and its magnitude is limited primarily by the horizontal grid resolution. If the full vertical velocity equation were being used, as in a nonhydrostatic model, the other terms in the vertical momentum equation would act to limit the vertical velocities.

Another example is that of propagating internal waves. Large amplitude internal waves tend to steepen as they propagate due to amplitude dispersion. Solitons form due to a balance between the steepening effect of amplitude dispersion and the countering effect of frequency dispersion in which shorter waves travel more slowly than longer waves. Hydrostatic models do not account for frequency dispersion; hence, they cannot simulate the formation of soliton waves.

Nonhydrostatic phenomena can have scales as large as several km. For example, internal soliton waves can have horizontal wavelengths of a couple of km. But this is not to say that hydrostatic models cannot be used to simulate flows at small horizontal scales, just that certain processes in which vertical accelerations are important may not be correctly simulated. Such processes are frequently secondary in importance to investigating the variability of the horizontal flow, a task for which the hydrostatic model generally provides useful results.

4.2 Sigma Vertical Coordinates

Sigma coordinates provide several advantages in modeling coastal regions including the ability to accurately represent the bathymetry (given sufficient horizontal resolution), a smooth treatment of bottom-following flows, the ability to provide increased resolution and a fairly consistent grid in the bottom boundary layer, and increased vertical resolution in shallower water (which may be desirable if the focus of the modeling is nearshore processes). The major problems with using sigma coordinates stem from inadequate resolution of steep slopes. In such situations, the horizontal pressure gradient, advection, and mixing terms can all generate significant truncation errors. Note that "steep slope" here is a relative term and can refer to a ship channel in a bay in a high-resolution simulation as well as a continental slope or a seamount in a larger scale simulation.

As noted in Section 3.2, the horizontal pressure gradient between two points in sigma coordinates is calculated as the difference between two terms, one being the pressure gradient along the sigma layer and the other being the vertical pressure gradient due to any difference in depth between the two points. For a steeply sloping sigma layer, the vertical pressure difference can be quite large and the net horizontal pressure gradient becomes the difference between two large terms, a situation in which numerical truncation errors can become significant. Subtracting off a mean

vertical density gradient, as is usually done and is discussed in Section 3.2, helps considerably, but truncation errors can still be significant.

Haney (1991) discussed the "hydrostatic consistency" problem with the horizontal pressure gradient in sigma coordinates. The degree of this problem is defined by the number of sigma layers that are crossed when traversing between adjacent horizontal points at a particular depth. If a number of layers are crossed, the pressure gradient that is calculated may not properly represent the actual density changes since the changes are not being resolved in the calculation. Haney argued that it was undesirable to cross more than one sigma layer boundary between adjacent horizontal points at a fixed depth (it can be seen that this restriction tends to be most strongly felt in the deeper layers). This turns out to be a very strict limitation to which few modelers using sigma coordinates actually adhere.

A common measure of the severity of the bathymetry changes is defined as the change in depth between two adjacent horizontal points relative to the mean depth, i.e.,

$$\Gamma = \left| \frac{H_x - H_{x-\Delta x}}{\frac{1}{2}(H_x + H_{x-\Delta x})} \right|. \tag{110}$$

Haney's hydrostatic consistency limitation for the bottom layer of a sigma coordinate model can be expressed approximately as

$$\Gamma_b = \left| \frac{H_x - H_{x-\Delta x}}{\Delta\sigma_b \frac{1}{2}(H_x + H_{x-\Delta x})} \right|, \tag{111}$$

where $\Delta\sigma_b$ is the fractional thickness of the bottom sigma layer. Hence, $\Gamma_b = \Gamma/\Delta\sigma_b$. According to Haney (1991), we need Γ_b less than about 1. Sigma coordinate modelers frequently use a criterion of $\Gamma \leq 1.5$ or more, which for typical values of $\Delta\sigma_b$ of 0.2 or less is a significant violation of Haney's hydrostatic consistency criteria.

Martin et al. (1998) discussed problems with advection and diffusion along sloping sigma surfaces when using sigma coordinates. A problem that can occur with the advection term in regions of steep slopes is that two adjacent points within a sigma layer may lie on different sides of a thermocline or halocline. In this case, the temperature or salinity field appears as a sharp front to the horizontal advection term. If there is persistent advection across this front using the second-order, centered advection scheme, there will be what is referred to as an "advective overshoot" on the upstream side of the front. Such an overshoot can reach about one third the magnitude of the jump across the front and can result in the model calculation becoming unstable. The problem is that the front is not adequately resolved. The second-order, centered advection scheme requires a front to be resolved by at least a few gridpoints to avoid significant advective overshoots. The remedy in this case is to increase the horizontal grid resolution or reduce the steepness of the bottom slope so that the fronts are better resolved.

As illustrated by Paul (1994), diffusion along sloping sigma layers can effectively act as vertical diffusion. Since horizontal mixing in ocean models is typically much larger than vertical mixing, the strong diffusion along a sloping sigma layer can result in excessive vertical diffusion and can excessively erode vertical gradients. The practice of calculating the diffusive fluxes using the anomaly based on some mean or climatological field (Section 3.2) significantly reduces this spurious vertical

diffusion. However, if there is a large, local anomaly relative to the mean field being subtracted off, significant spurious diffusion can still occur. For example, in an area of downwelling near a coast there will be a warm anomaly, which can spuriously warm the shallower water closer to the coast by diffusion of heat along the sigma layers. This problem can be reduced by accounting for the anomaly in the mean field being used as a reference (which may require updating the mean field periodically), by increasing the horizontal grid resolution, or by decreasing the bottom slope.

The common answer in dealing with sigma coordinate problems over steep slopes is to increase the horizontal grid resolution to better resolve the slope or to (artificially) reduce the severity of the slope. As noted by Haney (1991) and others, increasing vertical resolution does not help and can even make the problem worse. What the maximum slopes are that can be tolerated in sigma coordinates is not clear, probably because the answer is somewhat situation dependent. Modelers typically modify their bottom slopes as little as possible when trying to alleviate apparent sigma coordinate problems, so that they maintain the most accurate possible bathymetry. However, it is not always easy to discern whether or not steep slope areas are causing spurious results. In some cases, running grid convergence tests or comparing against a different (e.g., z-level) vertical coordinate simulation may be the only way to determine if there is a problem.

4.3 Z-level Vertical Coordinates

The z-level grid in NCOM truncates the bottom depth to the nearest model level. This is the simplest way to implement a z-level grid in an ocean model but, with such a treatment, the accuracy of the representation of the bathymetry in the model depends on the vertical grid resolution that is used. Martin et al. (1998) discussed some of the problems resulting from the use of such a z-level grid. Basically, the model generates the solution for the stepwise bathymetry that is used in the model rather than for the actual bathymetry. This may sound obvious, but modelers tend to think in terms of the bathymetry they are representing rather than the actual bathymetry being used in the model.

The effects of a stepwise bathymetry are readily noticeable in a barotropic onshore or offshore flow (Martin et al. 1998). The convergence of the horizontal flow occurs at the faces of the bathymetry steps, which produces a vertical velocity "jet" at the faces of the steps. If the steps were actually there, this would be the correct solution. However, if the steps represent an approximation to a smoothly varying bottom depth, the vertical velocity field will not vary smoothly in the horizontal as it should. Increased vertical resolution helps to reduce this problem. A better solution would be to truncate the bottom grid cells on the z-level grid to the bathymetry.

Since the z-level grid follows level surfaces, advection and diffusion along the z-levels are directed horizontally. If isopycnal surfaces depart from the horizontal plane, horizontal diffusion along the level surfaces can result in excessive cross-isopycnal diffusion. This tends to be less of a problem than diffusion along steeply sloping sigma layers, but it can still be a problem, especially on longer timescales as the effects of spurious diffusion increase. Simulations of basin-scale circulation with z-level models have had trouble with this, which has spurred the development and use of isopycnal coordinate models (Bleck et al. 1992).

4.4 Implicit Treatment of the Free Surface

The implicit treatment of surface waves used in NCOM is not as accurate as the split-explicit scheme used by POM. This is mainly because of the much larger timestep used with the implicit scheme. The error in propagating surface waves involves both damping and phase speed error (Martin et al. 1998).

NCOM provides user-selectable temporal weightings for the surface elevation gradients in the momentum equations and the divergence terms in the depth-averaged continuity equation, which are the principal terms involved in surface wave propagation (Section 3.6). Dukowicz and Smith (1994) discuss selecting weightings for these terms for an implicit treatment of the free surface. Dukowicz and Smith used an equal weighting at the three time levels for the surface elevation gradients and a fully implicit weighting (i.e., fully at time level $n+1$) for the divergence terms. This was based on a compromise between accuracy and noise damping requirements for their large-scale simulations. The Estuarine and Coastal Ocean Model, Semi Implicit (ECOM-si) version (Blumberg 1992) uses a fully implicit treatment of both sets of terms; however, this treatment results in strong damping of the surface waves (Martin et al. 1998). The NRL Layered Ocean Model (NLOM) (Wallcraft 1991) uses an even split between the old and new time levels.

The minimum damping of surface waves with the implicit scheme can be obtained by using the same temporal weighting at the old and new time levels for the surface pressure gradient and depth-averaged divergence terms in the free-surface Eqs. (86) to (88). With this weighting, there is no damping by the leapfrog scheme itself; the damping is due only to the Asselin filter (Martin et al. 1998). The damping from the Asselin filter can be reduced by reducing the Asselin filter coefficient; however, the filter coefficient must be kept large enough to suppress timesplitting. If the damping of the surface waves must be reduced further or if the phase speed error for the propagation of the surface waves must be decreased, then the model timestep must be reduced.

4.5 Second-Order Centered Advection

As already mentioned, the second-order centered advection scheme suffers from advective overshoots at sharp fronts. This scheme assumes that the field being advected varies smoothly in space and that significant gradients are resolved by at least a few points. The advantages of this scheme are that it is simple, computationally efficient, and gives fairly good accuracy when the gradients are well-resolved. This scheme has certainly been used more than any other in ocean models (e.g., in the Bryan-Cox model (Bryan 1969), POM (Blumberg and Mellor 1987), NLOM (Wallcraft 1991), and many others).

Other problems with the second-order centered advection scheme that are related to the overshooting problem are that it does not maintain the monotonicity, extrema, or positive definiteness of the advected field. These are sometimes desirable properties, e.g., salinity and biological constituents being advected by an ocean model should not, in principle, take on negative values.

The second-order centered advection scheme usually requires a certain amount of horizontal diffusion to maintain smooth solutions in strongly advective flows. This need is addressed fairly directly by the grid-cell Reynolds number horizontal mixing parameterization (Section 2.4). Using a small value of the grid-cell Reynolds number (e.g., 10) usually maintains a smooth solution but

tends to significantly damp the flow and dissipate sharp gradients. Using a larger value (e.g., 100) results in much less damping but can result in a significant amount of small-scale noise. The Smagorinsky mixing scheme is less directly pointed at filtering numerical noise, but as a practical matter, the extent to which it suppresses noise and damps the flow can be regulated by changing the value of its scaling parameter C_{smag} (Section 2.4).

There are different philosophies regarding the presence of small-scale noise in a numerical model simulation. One philosophy is that all such noise is objectionable. Another is that that there is a fair amount of noise in the real ocean anyway and, as long as the dynamical processes being simulated are not significantly affected, a certain amount of noise is tolerable.

4.6 Timestep Limitations

A basic principle for the stability of explicit numerical schemes (at least those being used in NCOM) is that a signal (i.e., the propagation of a wave or the advection or diffusion of a field) cannot travel more than a single grid interval in a single timestep. The processes that limit the timestep used in NCOM are internal wave propagation, horizontal and vertical advection, and horizontal mixing. Since the surface waves and vertical mixing are treated implicitly, they are not subject to a timestep limitation with regard to numerical stability.

The speed of internal waves depends on the vertical density stratification and the depth. In the deep ocean, the maximum speed of internal waves is typically 2 to 3 m/s. In coastal areas, where the water is relatively shallow and the stratification tends to be weaker, the maximum internal wave speeds are usually less than 1 m/s. The horizontal advection speeds depend on the situation (e.g., on the strength of the tidal currents and the winds) but are typically less than 2 m/s and may be less than 1 m/s in weakly forced situations. In general, the maximum speeds for internal wave propagation and advection tend to be comparable.

Vertical advection is another matter. If one is trying to use high vertical resolution, vertical advection can be the limiting factor in setting the timestep. With sigma coordinates, the vertical grid spacing is reduced in shallow water and this reduced grid spacing may limit the timestep. The use of a stretched vertical grid with higher vertical resolution at the surface and/or bottom (on a sigma coordinate grid) and lower resolution at mid depth helps the situation since the vertical velocity must go to zero at the free surface and at the bottom. Another factor that helps this situation is that vertical mixing in shallow water due to winds and bottom drag helps suppress the generation of vertical motion relative to the sigma surfaces.

Horizontal diffusion is almost never a factor in setting the timestep since the horizontal diffusive time scale necessary to achieve smooth solutions is usually much smaller than the advective and internal wave timestep restrictions.

For coastal simulations, a conservative estimate of the maximum internal wave and advection speeds is generally about 2 m/s. With 2 m/s as a maximum velocity, the maximum allowable timestep for NCOM for a 1-km grid would be about 250 s (the effective timestep for the leapfrog scheme is $2\Delta t$). For a larger or smaller grid spacing, the maximum timestep would change proportionally. Note that these numbers just provide an approximate value. Vertical advective processes may require a smaller timestep, and it is possible for wave and advective speeds to combine to

generate larger effective signal velocities than either advection or wave propagation considered separately.

Another consideration for the timestep, besides stability, is accuracy. Because the advection, baroclinic pressure gradient, and Coriolis terms are treated explicitly and are centered in time with the leapfrog scheme, temporal truncation errors are small and temporal accuracy is quite good as long as the timestep is sufficiently small that the numerical scheme remains stable (and the inertial period is well-resolved for the Coriolis term). Since surface waves and vertical mixing are treated implicitly, their temporal accuracy must be given separate consideration.

The accuracy of the implicit treatment of the free surface is discussed in Section 4.4. The damping of surface waves can be minimized for a given timestep by appropriate selection of model parameter values. Further reduction of surface wave damping and/or reduction of the surface wave phase speed error requires decreasing the timestep.

The fully implicit treatment of vertical mixing is subject to temporal truncation error. In most conditions, this error in the mixing rate is small and is not especially noticeable since vertical mixing tends to be fairly rapid relative to the usual timescales of concern. (There is also the point that the rate of vertical mixing is probably not simulated very accurately anyway due to the lack of a physical model that correctly accounts for all the significant processes involved.) However, in cases with very large vertical mixing coefficients (e.g., strong winds) and fine vertical resolution, it is possible to have sufficient temporal truncation error in the vertical mixing such that spurious mixing occurs. Such spurious mixing effects were observed in some idealized forcing experiments where high vertical resolution was used but have not been noticed in any realistic model similations to date. It is planned to investigate this mixing problem more thoroughly.

4.7 Drying of Grid Cells

If the surface elevation reaches the bottom of a grid cell or the bottom of the sigma coordinate grid (z_σ), NCOM will "blow up." This is sometimes the reason why an otherwise smoothly running simulation suddenly stops. To keep this from happening, the minimum depth of the model grid cells (or z_σ) must be set deeper than the minimum depth of the free surface expected at that location. Of course, one doesn't always know what the minimum depth of the free surface will be, so that an educated (conservative) guess may be needed when initially setting the minimum depths for a particular simulation.

5. PLANS

For future development of NCOM, it is planned to address some of the limitations discussed in the previous section. Some enhancements that are being considered are as follows:

- Provide the option for an advection scheme that provides some degree of upwinding at fronts to avoid or reduce the overshooting problems of the second-order centered scheme. A number of ocean modelers have begun using advection schemes that use some degree of upwinding at fronts to avoid or reduce advective overshoots. Many schemes have been discussed in the literature (Rood 1987; Pietrzak 1995), and the different schemes have particular advantages and disadvantages. They all tend to involve significantly more computation than the second-order centered scheme.

- Truncate the bottom grid cell to the bathymetry on the z-level grid to more accurately represent the bottom depth.
- Implement a flooding and drying scheme. This would provide several benefits including (a) preventing the accidental drying out of a grid cell from prematurely terminating a model run, (b) providing more accurate simulations in shallow coastal areas by allowing depths and land-sea boundaries to be set without being restricted by the need to avoid grid cells drying out, and (c) providing the ability of the model to accurately simulate the flooding/drying process itself (if an accurate flooding/drying scheme based on correct physics is developed).

6. SUMMARY

This report provides a description of NCOM Version 1.0. The model has a free surface and is based on the primitive equations and the hydrostatic, Boussinesq, and incompressible approximations. A choice of a grid-cell Reynolds number or the Smagorinsky scheme is provided for horizontal mixing, and a choice of the MYL2 or MYL2.5 turbulence models is provided for the parameterization of vertical mixing. An option is also provided to include the vertical mixing enhancement scheme of Large et al. (1994) to parameterize unresolved mixing processes occurring at near-critical Richardson numbers. The inclusion of a source term in the model equations simplifies input of river and runoff inflows.

The model uses an Arakawa C grid, is leapfrog in time with an Asselin filter to suppress timesplitting, and uses second-order centered spatial finite differences. The propagation of surface waves and vertical diffusion are treated implicitly. The horizontal grid is curvilinear. The vertical grid uses sigma coordinates for the upper layers and z-level (constant depth) coordinates for the lower layers, and the depth at which the model changes from sigma to z-level coordinates can be specified by the user by setting a single parameter. The combined vertical coordinate system provides some flexibility in setting up the vertical grid and easily allows comparisons to be made between simulations conducted with sigma and z-level coordinates.

The model is based on fairly well-tested ocean model physics and numerics. However, there are a number of limitations of the model. Some of these are mentioned here (the model's limitations are discussed in more detail in Section 4).

Since the model is hydrostatic, vertical motions on small horizontal scales may not be properly described. This does not prevent the model from being applied with high horizontal resolution to look at the structure of predominantly horizontal flows. However, nonhydrostatic processes that can occur in these situations will not be correctly simulated.

Sigma coordinates can accurately represent the changing bottom depth but can suffer from truncation errors in their horizontal advection, diffusion, and baroclinic pressure gradient terms if steep bottom slopes are not adequately resolved. The solution to this problem is to increase the horizontal grid resolution or artificially decrease the severity of the slope.

The z-level grid does not suffer from these problems but has limitations of its own. Since the z-level grid used in NCOM truncates the bathymetry to the nearest z-level, the accuracy of the representation of the bathymetry on the z-level grid depends on the vertical grid resolution, and the stepwise structure of the z-level grid can cause some distortion of flows that cross the steps.

Also, the z-level grid does not provide very consistent resolution in the bottom boundary layer unless a large number of levels are used over the depth range at which the bottom boundary layer exists.

The second-order centered advection scheme provides fairly good accuracy for advection of fields in which the gradients are moderately well-resolved but can generate advective overshoots at sharp fronts. In setting the timestep for the model, the timestep limitation for the propagation of internal waves and for horizontal and vertical advection must not be exceeded or numerical instability may result. Also, the drying out of a grid cell due to depression of the free surface to the sea bottom in shallow water or the bottom of the sigma grid can cause a model simulation to suddenly terminate.

7. ACKNOWLEDGMENTS

This work was sponsored by the Office of Naval Research through the Ocean Model Development for COAMPS Task of the Naval Ocean Modeling and Prediction Program (Program Element 602435N).

8. REFERENCES

Asselin, R., 1972: Frequency filter for time integrations. *Mon. Wea. Rev., 100*, 487-490.

Bleck, R., C. Rooth, D. Hu, and L.T. Smith, 1992: Salinity-driven thermocline transients in a wind- and thermohaline-forced isopycnic coordinate model of the North Atlantic. *J. Phys Oceanogr., 22*, 1486-1505.

Blumberg, A.F. and G.L. Mellor, 1983: Diagnostic and prognostic numerical circulation studies of the South Atlantic Bight. *J. Geophys. Res., 88*, 4579- 4592.

Blumberg, A.F. and G.L. Mellor, 1987: A description of a three-dimensional coastal ocean circulation model. In *Three-Dimensional Coastal Ocean Models*, N. Heaps, Ed., American Union, New York, N.Y., 208 pp.

Blumberg, A.F., 1992: *A Primer for ECOM-si.* HydroQual, Inc., Mahwah, N.J., 64 pp.

Bryan, K., 1969: A numerical method for the study of the circulation of the World Ocean. *J. Comput. Phys., 4*, 347-376.

Casulli, V. and E. Cattani, 1994: Stability, accuracy, and efficiency of a semi-implicit method for three-dimensional shallow water flow. *Computers and Mathematics with Applications, 27*, 99-112.

Casulli, V. and R.T. Cheng, 1994: Solutions of primitive equations for three-dimensional tidal circulation. In *Estuarine and Coastal Modeling III, Proceedings of the 3rd International Conference*, ASCE, New York, N.Y., 396-406.

Casulli, V. and G.S. Stelling, 1996: Simulation of three-dimensional, non-hydrostatic free-surface flows for estuaries and coastal seas. In *Estuarine and Coastal Modeling, Proceedings of the 4th International Conference*, M.L. Spaulding and R.T. Cheng, Eds., American Society of Civil Engineers, New York, N.Y., 1-25.

Craig, P.D. and M.L. Banner, 1994: Modeling wave-enhanced turbulence in the ocean surface layer. *J. Phys. Oceanogr., 24*, 2546-2559.

Craig, P.D., 1996: Velocity profiles and surface roughness under breaking waves. *J. Geophys. Res., 101*, 1265-1277.

Dietrich, D.E. and D.S. Ko, 1994: A semi-collocated ocean model based on the SOMS approach. *Int. J. Num. Methods in Fluids, 19*, 1103-1113.

Dukowicz, J.K. and R.D. Smith, 1994: Implicit free-surface method for the Bryan-Cox-Semtner ocean model. *J. Geophys. Res., 99*, 7991-8014.

Friedrich, H. and S. Levitus, 1972: An approximation to the equation of state for sea water, suitable for numerical ocean models. *J. Phys. Oceanogr., 2*, 514-517.

Haney, R.L., 1974: A numerical study of the response of an idealized ocean to large-scale surface heat and momentum flux. *J. Phys. Oceanogr., 4*, 145-167.

Haney, R.L., 1991: On the pressure gradient force over steep topography in sigma coordinate ocean models. *J. Phy. Oceanogr., 21*, 610-619.

Hodur, R.M., 1997: The Naval Research Laboratory's Coupled Ocean/Atmosphere Mesoscale Prediction System (COAMPS). *Mon. Wea. Rev., 125*, 1414-1430.

Hurlburt, H.E. and J.D. Thompson, 1980: A numerical study of Loop Current intrusions and eddy shedding. *J. Phys. Oceanogr., 10*, 1611-1651.

Kantha L.H. and C.A. Clayson, 1994: An improved mixed layer model for geophysical applications. *J. Geophys. Res., 99*, 25235-25266.

Killworth, P.D., D. Stainforth, D.J. Webb, and S.M. Paterson, 1991: The development of a free-surface Bryan-Cox-Semtner ocean model. *J. Phys. Oceanogr., 21*, 1333-1348.

Large, W.G., J.C. McWilliams, and S. Doney, 1994: Oceanic vertical mixing: a review and a model with a nonlocal boundary layer parameterization. *Rev. Geophys., 32*, 363-403.

Leendertse, J.J., 1989: A new approach to three-dimensional free-surface flow modeling. The RAND Corporation Memorandum R-3712-NETH/RC, Santa Monica, Calif.

Martin, P.J., 1985: Simulation of the ocean mixed layer at OWS November and Papa with several models. *J. Geophys. Res., 90*, 903-916.

Martin, P.J., 1986: Testing and Comparison of Several Mixed-Layer Models. NORDA Report 143. Naval Research Laboratory, Stennis Space Center, Miss., 30 pp.

Martin, P.J., G. Peggion, and K.J. Yip, 1998: A comparison of several coastal ocean models. NRL Report NRL/FR/7322--97-9692. Naval Research Laboratory, Stennis Space Center, Miss., 96 pp.

Mellor, G.L. and T. Yamada, 1974: A hierarchy of turbulence closure models for planetary boundary layers. *J. Atmos. Sci., 31*, 1791-1806.

Mellor, G.L. and P.A. Durbin, 1975: The structure and dynamics of the ocean surface mixed layer. *J. Phys. Oceanogr., 5*, 718-728.

Mellor, G.L. and T. Yamada, 1982: Development of a turbulence closure model for geophysical fluid problems. *Geophys. and Space Phys., 20*, 851-875.

Mellor, G.L. and A.F. Blumberg, 1985: Modeling vertical and horizontal diffusivities with the sigma coordinate system. *Mon. Wea. Rev., 113*, 1379-1383.

Mellor, G.L., 1991: An equation of state for numerical models of oceans and estuaries. *J. Atmos. and Ocean Tech., 8*, 609-611.

Mellor, G.L., 1996: *User's Guide for a Three-Dimensional, Primitive-Equation, Numerical Ocean Model.* Princeton University, Princeton, N.J., 39 pp.

Paul, J.F., 1994: Observations related to the use of the sigma coordinate transformation for estuarine and coastal modeling studies. In *Estuarine and Coastal Modeling III, Proceedings of the 3rd International Conference*, M. Spaulding, K. Bedford, A. Blumberg, R. Cheng, and C. Swanson, Eds., American Society of Civil Engineers, New York, N.Y., 682 pp.

Pietrzak, J.D., 1995: A comparison of advection schemes for ocean modelling. Report 95-8 of the Danish Meteorological Institute, Copenhagen, Denmark, 130 pp.

Rood, R.B., 1987: Numerical advection algorithms and their role in atmospheric transport and chemistry models. *Rev. Geophys., 25*, 71-100.

Smagorinsky, J., 1963: General circulation experiments with the primitive equations. I: The basic experiment. *Mon. Wea. Rev., 91*, 99-164.

Troen, I.B. and L. Mahrt, 1986: A simple model of the atmospheric boundary layer; sensitivity to surface evaporation. *Boundary Layer Meteorol., 37*, 129-148.

Wallcraft, A.J., 1991: The Navy Layered Ocean Model Users' Guide. NOARL Report 35, Naval Research Laboratory, Stennis Space Center, Miss., 21 pp.

Appendix A

EQUATIONS IN ORTHOGONAL, CURVILINEAR, HORIZONTAL COORDINATES

The derivation of vector differential expressions in orthogonal, curvilinear coordinates is discussed in Batchelor (1970). The form of the basic equations in orthogonal, curvilinear, horizontal coordinates is taken from Blumberg and Herring (1987) and Song and Haidvogel (1994). The notation used here is similar to that used by Batchelor and by Blumberg and Herring.

Let the new horizontal coordinates be ξ_1 and ξ_2 and let $\mathbf{a}$ and $\mathbf{b}$ be unit vectors parallel to ξ_1 and ξ_2, respectively. Then the change in the horizontal position vector $\mathbf{x}$ corresponding to increments in ξ_1 and ξ_2 is

$$\delta\mathbf{x} = h_1\delta\xi_1\mathbf{a} + h_2\delta\xi_2\mathbf{b}, \tag{A1}$$

where h_1 and h_2 are metric coefficients that scale the distance along the coordinate axes and are functions of ξ_1 and ξ_2.

The horizontal velocities in the new coordinate system are defined (for convenience) to be u and v and are directed along ξ_1 and ξ_2, respectively, i.e.,

$$u = h_1\frac{d\xi_1}{dt}, \tag{A2}$$

$$v = h_2\frac{d\xi_2}{dt}. \tag{A3}$$

The basic, 3-D Eqs. (1) to (6) in the new horizontal coordinate system become

$$\begin{aligned}\frac{\partial u}{\partial t} = &-\frac{1}{h_1h_2}\frac{\partial}{\partial\xi_1}(h_2uu) - \frac{1}{h_1h_2}\frac{\partial}{\partial\xi_2}(h_1vu) - \frac{\partial}{\partial z}(wu) + Qu \\ &+\left(f + \frac{1}{h_1h_2}\left(v\frac{\partial h_2}{\partial\xi_1} - u\frac{\partial h_1}{\partial\xi_2}\right)\right)v - \frac{1}{\rho_o h_1}\frac{\partial p}{\partial\xi_1} + F_u + \frac{\partial}{\partial z}\left(K_M\frac{\partial u}{\partial z}\right),\end{aligned} \tag{A4}$$

$$\begin{aligned}\frac{\partial v}{\partial t} = &-\frac{1}{h_1h_2}\frac{\partial}{\partial\xi_1}(h_2uv) - \frac{1}{h_1h_2}\frac{\partial}{\partial\xi_2}(h_1vv) - \frac{\partial}{\partial z}(wv) + Qv \\ &-\left(f + \frac{1}{h_1h_2}\left(v\frac{\partial h_2}{\partial\xi_1} - u\frac{\partial h_1}{\partial\xi_2}\right)\right)u - \frac{1}{\rho_o h_2}\frac{\partial p}{\partial\xi_2} + F_v + \frac{\partial}{\partial z}\left(K_M\frac{\partial v}{\partial z}\right),\end{aligned} \tag{A5}$$

$$\frac{\partial p}{\partial z} = -\rho g, \tag{A6}$$

$$\frac{1}{h_1 h_2}\frac{\partial(h_2 u)}{\partial \xi_1} + \frac{1}{h_1 h_2}\frac{\partial(h_1 v)}{\partial \xi_2} + \frac{\partial w}{\partial z} = Q, \tag{A7}$$

$$\begin{aligned}\frac{\partial T}{\partial t} = &-\frac{1}{h_1 h_2}\frac{\partial}{\partial \xi_1}(h_2 u T) - \frac{1}{h_1 h_2}\frac{\partial}{\partial \xi_2}(h_1 v T) - \frac{\partial}{\partial z}(wT) + QT \\ &+ \frac{1}{h_1 h_2}\frac{\partial}{\partial \xi_1}\left(A_H \frac{h_2}{h_1}\frac{\partial T}{\partial \xi_1}\right) + \frac{1}{h_1 h_2}\frac{\partial}{\partial \xi_2}\left(A_H \frac{h_1}{h_2}\frac{\partial T}{\partial \xi_2}\right) + \frac{\partial}{\partial z}\left(K_H \frac{\partial T}{\partial z}\right) \\ &+ Q_r \frac{\partial \gamma}{\partial z},\end{aligned} \tag{A8}$$

$$\begin{aligned}\frac{\partial S}{\partial t} = &-\frac{1}{h_1 h_2}\frac{\partial}{\partial \xi_1}(h_2 u S) - \frac{1}{h_1 h_2}\frac{\partial}{\partial \xi_2}(h_1 v S) - \frac{\partial}{\partial z}(wS) + QS \\ &+ \frac{1}{h_1 h_2}\frac{\partial}{\partial \xi_1}\left(A_H \frac{h_2}{h_1}\frac{\partial S}{\partial \xi_1}\right) + \frac{1}{h_1 h_2}\frac{\partial}{\partial \xi_2}\left(A_H \frac{h_1}{h_2}\frac{\partial S}{\partial \xi_2}\right) + \frac{\partial}{\partial z}\left(K_H \frac{\partial S}{\partial z}\right).\end{aligned} \tag{A9}$$

These equations in curvilinear horizontal coordinates look very similar to the original Eqs. (1) to (6) in Cartesian horizontal coordinates. The only additional terms that appear in the curvilinear equations above are the curvature correction terms for advection in the momentum equations, i.e., the term

$$+\frac{1}{h_1 h_2}\left(v\frac{\partial h_2}{\partial \xi_1} - u\frac{\partial h_1}{\partial \xi_2}\right) v \tag{A10}$$

in the equation for u and the term

$$-\frac{1}{h_1 h_2}\left(v\frac{\partial h_2}{\partial \xi_1} - u\frac{\partial h_1}{\partial \xi_2}\right) u \tag{A11}$$

in the equation for v. These terms account for the interchange of u and v momentum for advection along a curvilinear grid. Since u and v are directed along the horizontal coordinates ξ_1 and ξ_2, momentum advection along these coordinates will effectively result in conversion of momentum between u and v if the coordinates have non-zero curvature. Note that the advective curvature correction terms in Eqs. (A4) and (A5) are combined with the Coriolis terms since they have a similar form.

The Smagorinsky horizontal mixing terms for momentum, given by Eqs. (25) and (26), when converted to curvilinear coordinates, have the form (Blumberg and Herring 1987)

$$F_u = \frac{1}{h_1 h_2}\left(\frac{\partial(h_2 \tau_{11})}{\partial \xi_1} + \frac{\partial(h_1 \tau_{21})}{\partial \xi_2} + \tau_{21}\frac{\partial h_1}{\partial \xi_2} - \tau_{22}\frac{\partial h_2}{\partial \xi_1}\right) \tag{A12}$$

and

$$F_v = \frac{1}{h_1 h_2}\left(\frac{\partial(h_2 \tau_{12})}{\partial \xi_1} + \frac{\partial(h_1 \tau_{22})}{\partial \xi_2} + \tau_{12}\frac{\partial h_2}{\partial \xi_1} - \tau_{11}\frac{\partial h_1}{\partial \xi_2}\right), \tag{A13}$$

where

$$\tau_{11} = 2A_M\left(\frac{1}{h_1}\frac{\partial u}{\partial \xi_1} + \frac{v}{h_1 h_2}\frac{\partial h_1}{\partial \xi_2}\right), \tag{A14}$$

$$\tau_{22} = 2A_M \left(\frac{1}{h_2} \frac{\partial v}{\partial \xi_2} + \frac{u}{h_1 h_2} \frac{\partial h_2}{\partial \xi_1} \right), \tag{A15}$$

$$\tau_{12} = \tau_{21} = A_M \left(\frac{h_2}{h_1} \frac{\partial}{\partial \xi_1} \left(\frac{v}{h_2} \right) + \frac{h_1}{h_2} \frac{\partial}{\partial \xi_2} \left(\frac{u}{h_1} \right) \right). \tag{A16}$$

The form of the terms for the grid-cell Reynolds number horizontal diffusion in curvilinear coordinates is analogous. The terms involving $\frac{\partial h_2}{\partial \xi_1}$ and $\frac{\partial h_1}{\partial \xi_2}$ in Eqs. (A4) and (A5) are curvature correction terms for the horizontal mixing of momentum. These terms are assumed to be small and are not included in POM (Mellor 1996) or NCOM.

Note that when converting the equations to finite difference form with second-order centered differences, we set

$$\frac{1}{h_1} \frac{\partial \phi}{\partial \xi_1} = \frac{1}{h_1 \Delta \xi_1} \delta_{\xi_1} \phi, \tag{A17}$$

where

$$\delta_{\xi_1} \phi = \phi_{\xi_1 + \Delta \xi_1/2} - \phi_{\xi_1 - \Delta \xi_1/2}. \tag{A18}$$

If x' is taken to be the arc length in the ξ_1 direction and $h_1 \Delta \xi_1 = \Delta x'$ is taken to be the grid spacing in the ξ_1 direction and then the primes on x are dropped, then

$$\frac{1}{h_1} \frac{\partial \phi}{\partial \xi_1} = \frac{1}{\Delta x} \delta_x \phi. \tag{A19}$$

Similarly,

$$\frac{1}{h_1 h_2} \frac{\partial (h_2 u \phi)}{\partial \xi_1} = \frac{1}{h_1 \Delta \xi_1 h_2 \Delta \xi_2} \delta_{\xi_1} (h_2 \Delta \xi_2 u \phi) = \frac{1}{\Delta x \Delta y} \delta_x (\Delta y^u u \phi), \tag{A20}$$

where Δy and Δy^u are the grid spacing in the ξ_2 direction at a grid-cell center and at a u-point, respectively. In deriving finite difference expressions such as in Eq. (A20), use is made of the fact that $\Delta \xi_1$ and $\Delta \xi_2$ in the transformed coordinate system are constants (i.e., variations in the grid spacing are accounted for in the metric coefficients h_1 and h_2).

A1. REFERENCES

Batchelor, G.K., 1970: *An Introduction to Fluid Dynamics.* Cambridge University Press, New York, N.Y., 615 pp.

Blumberg, A.F. and H.J. Herring, 1987: Circulation modeling using orthogonal curvilinear coordinates. In *Three-Dimensional Models of Marine and Estuarine Dynamics*, J.C. Nihoul and B.M. Jamart, Eds., Elsevier Oceanography Series, *45*.

Mellor, G.L., 1996: *User's Guide for a Three-Dimensional, Primitive-Equation, Numerical Ocean Model.* Princeton University, Princeton, N.J., 39 pp.

Song, Y. and D. Haidvogel, 1994: A semi-implicit ocean circulation model using a generalized topography-following coordinate system. *J. Comput. Phys., 115*, 2428-2441.

Appendix B

EQUATIONS IN SIGMA VERTICAL COORDINATES

The basic, 3-D model equations written in curvilinear horizontal coordinates and sigma vertical coordinates are (Blumberg and Herring 1987)

$$\begin{aligned}\frac{1}{D_\sigma}\frac{\partial D_\sigma u}{\partial t} = &-\frac{1}{h_1 h_2 D_\sigma}\frac{\partial}{\partial \xi_1}(h_2 D_\sigma uu) - \frac{1}{h_1 h_2 D_\sigma}\frac{\partial}{\partial \xi_2}(h_1 D_\sigma vu) \\ &- \frac{1}{D_\sigma}\frac{\partial}{\partial \sigma}(\omega u) + Qu + \left(f + \frac{1}{h_1 h_2}\left(v\frac{\partial h_2}{\partial \xi_1} - u\frac{\partial h_1}{\partial \xi_2}\right)\right)v \\ &- \frac{1}{\rho_o h_1}\frac{\partial p}{\partial \xi_1} + F'_u + \frac{1}{D_\sigma^2}\frac{\partial}{\partial \sigma}\left(K_M\frac{\partial u}{\partial \sigma}\right), \end{aligned} \tag{B1}$$

$$\begin{aligned}\frac{1}{D_\sigma}\frac{\partial D_\sigma v}{\partial t} = &-\frac{1}{h_1 h_2 D_\sigma}\frac{\partial}{\partial \xi_1}(h_2 D_\sigma uv) - \frac{1}{h_1 h_2 D_\sigma}\frac{\partial}{\partial \xi_2}(h_1 D_\sigma vv) \\ &- \frac{1}{D_\sigma}\frac{\partial}{\partial \sigma}(\omega v) + Qv - \left(f + \frac{1}{h_1 h_2}\left(v\frac{\partial h_2}{\partial \xi_1} - u\frac{\partial h_1}{\partial \xi_2}\right)\right)u \\ &- \frac{1}{\rho_o h_2}\frac{\partial p}{\partial \xi_2} + F'_v + \frac{1}{D_\sigma^2}\frac{\partial}{\partial \sigma}\left(K_M\frac{\partial v}{\partial \sigma}\right), \end{aligned} \tag{B2}$$

$$\frac{\partial p}{\partial z} = -\rho g, \tag{B3}$$

$$\frac{1}{D_\sigma}\frac{\partial D_\sigma}{\partial t} + \frac{1}{h_1 h_2 D_\sigma}\frac{\partial (h_2 D_\sigma u)}{\partial \xi_1} + \frac{1}{h_1 h_2 D_\sigma}\frac{\partial (h_1 D_\sigma v)}{\partial \xi_2} + \frac{1}{D_\sigma}\frac{\partial w}{\partial \sigma} = Q, \tag{B4}$$

$$\begin{aligned}\frac{1}{D_\sigma}\frac{\partial D_\sigma T}{\partial t} = &-\frac{1}{h_1 h_2 D_\sigma}\frac{\partial}{\partial \xi_1}(h_2 D_\sigma uT) - \frac{1}{h_1 h_2 D_\sigma}\frac{\partial}{\partial \xi_2}(h_1 D_\sigma vT) \\ &- \frac{1}{D_\sigma}\frac{\partial}{\partial \sigma}(\omega T) + QT + \frac{1}{h_1 h_2 D_\sigma}\frac{\partial}{\partial \xi_1}\left(A_H\frac{h_2 D_\sigma}{h_1}\frac{\partial T}{\partial \xi_1}\right) \\ &+ \frac{1}{h_1 h_2 D_\sigma}\frac{\partial}{\partial \xi_2}\left(A_H\frac{h_1 D_\sigma}{h_2}\frac{\partial T}{\partial \xi_2}\right) + \frac{1}{D_\sigma^2}\frac{\partial}{\partial \sigma}\left(K_H\frac{\partial T}{\partial \sigma}\right) + \frac{Q_r}{D_\sigma}\frac{\partial \gamma}{\partial \sigma}, \end{aligned} \tag{B5}$$

$$\begin{aligned}\frac{1}{D_\sigma}\frac{\partial D_\sigma S}{\partial t} = &-\frac{1}{h_1 h_2 D_\sigma}\frac{\partial}{\partial \xi_1}(h_2 D_\sigma uS) - \frac{1}{h_1 h_2 D_\sigma}\frac{\partial}{\partial \xi_2}(h_1 D_\sigma vS) \\ &- \frac{1}{D_\sigma}\frac{\partial}{\partial \sigma}(\omega S) + QS + \frac{1}{h_1 h_2 D_\sigma}\frac{\partial}{\partial \xi_1}\left(A_H\frac{h_2 D_\sigma}{h_1}\frac{\partial S}{\partial \xi_1}\right) \\ &+ \frac{1}{h_1 h_2 D_\sigma}\frac{\partial}{\partial \xi_2}\left(A_H\frac{h_1 D_\sigma}{h_2}\frac{\partial S}{\partial \xi_2}\right) + \frac{1}{D_\sigma^2}\frac{\partial}{\partial \sigma}\left(K_H\frac{\partial S}{\partial \sigma}\right), \end{aligned} \tag{B6}$$

where F'_u and F'_v are the horizontal mixing terms for u and v momentum.

B1. REFERENCES

Blumberg, A.F. and H.J. Herring, 1987: Circulation modeling using orthogonal curvilinear coordinates. In *Three-Dimensional Models of Marine and Estuarine Dynamics*, J.C. Nihoul and B.M. Jamart, Eds., Elsevier Oceanography Series, *45*.